Code 1

NASA TMX 51764   Cat 27

ELECTROSTATIC THRUSTORS FOR SPACE PROPULSION,

PRESENT AND FUTURE

N64-24030

By William R. Mickelsen[†] and Harold R. Kaufman[‡]

Lewis Research Center
National Aeronautics and Space Administration
Cleveland, Ohio

INTRODUCTION

It is the purpose of this paper to show the present status of elec-

trostatic thrustors as a component of electric propulsion systems, to

describe in detail their major research and development problems, and to

discuss their possible future performance.

At present, the chemical rocket is man's only operational primary

propulsion system for space flight. Nuclear rockets and electric ro ʹs

consist only of paper schemes and preliminary experimental equipment. It

is clear, however, that if the performance of these propulsion systems

lives up to expectations their use will make possible many space missions

that are impractical with chemical rockets.

Electric-propulsion systems can be divided into three major parts:

the electric powerplant, the thrustor, and any power-conversion equipment

between the two. The requirement for electric-propulsion systems with

regard to weight and durability has been discussed recently in references

1 and 2. Electric rockets can be competitive in payload fraction with

---

[†]Chief, Electrostatic Propulsion Branch
[‡]Head, Electrostatic Thrustor Systems Section

nuclear rockets for Mars missions only if they achieve a specific mass of about 10 kg/kw or less. To be competitive in trip time as well as payload fraction, the electric-propulsion system should be about 5 kg/kw or less.

Most, if not all, of electric-propulsion-system mass is usually assumed to reside in the electric powerplant. Analytical studies have resulted in estimates of powerplant masses in the range from 1 to 6 kg/kw (refs. 3 to 9). The only operational space electric powerplants, however, are solar cells and thermoelectric systems with specific masses from 50 to 100 kg/kw - too heavy to match even the small payload fraction of chemical rockets. Reduction of this large gap between actual and required powerplant weights is the aim of a large current research and development program in the U.S. Since the electric thrustor is useless without a suitably lightweight electric powerplant, it must be assumed herein that this program will be successful.

The first portion of this paper is devoted to an examination of the present status of electrostatic thrustors with regard to their integration as a component in lightweight propulsion systems. An existing experimental thrustor is used as an example, and the effects of the performance of this thrustor on some space missions are determined.

From this examination, a number of shortcomings of existing thrustors become apparent. Reasons for these shortcomings are explained in terms of the basic physical processes for each of the thrustor types. Research and development programs on these problems are summarized.

This paper is based on reference 10, which contains considerable additional analysis and discussion.

THRUSTOR PERFORMANCE

To illustrate the performance and deficiencies of existing electro-static thrustors, the theoretical payload capacity of an electric rocket vehicle is shown in figure 1 for a one-way Mars orbiter mission starting in a low orbit about Earth and ending in a low orbit about Mars. The powerplant is assumed to have a specific mass of 4 kg/kw.

The upper curve in figure 1 represents the maximum theoretical pay-load for the assumption that both the thrustor and the power-conversion equipment have 100 percent efficiency and negligible mass. In addition, it is assumed that the thrustor is capable of operating with the contin-uously variable thrust required to maximize the payload during inter-planetary transfer (ref. 11). Since the power $\mathcal{P}$ is maintained con-stant, the specific impulse I must also vary continuously. The relation between thrust and specific impulse is given by:

$$\mathcal{P} = \frac{1}{2} F g_c I \tag{1}$$

where the specific impulse is defined as

$$I \equiv \frac{F}{g_c \dot{m}_{tot}} \tag{2}$$

F is the thrust, $\dot{m}_{tot}$ is the propellant mass flow rate, and g_c is the gravitational conversion factor. In the variable-thrust optimized trajectory (Irving-Blum), the specific impulse varies over a large range (e.g., 10:1) with the lowest specific impulse occurring in the planeto-centric phases (refs. 11 to 13). Since existing thrustors are not capable of efficient operation over the required range of specific impulse, an alternative trajectory, using constant specific impulse and thrust, with

an optimized coast period in the middle of the heliocentric phase may be used instead. The first loss in payload shown in figure 1 is due to use of such constant specific impulse trajectories. (This curve was calculated from information in ref. 14.)

The more advanced electrostatic thrustors require most of their power in the form of high-voltage direct current, while power is generally produced in the form of low-voltage alternating current. The power could, of course, be generated as high-voltage alternating current, so that only rectification is necessary. But a recent analysis (ref. 15) of power-conversion equipment in the 1000-kilowatt power range has shown that conventional low-voltage electromagnetic generators with transformers should have lower specific mass than high-voltage electrogenerators without transformers for voltages above 2400 volts. Since almost all thrustors require voltages higher than 2400 volts in the specific impulse range of interest, the high-voltage electromagnetic generator will not be considered further here. Information in reference 16 indicates that an electromagnetic generator power-conversion system might be developed from present technology with a specific mass of about 6 or 7 kg/kw for the 1 to 10 megawatt power level. With advanced technology, the analysis in reference 15 predicts a specific mass of about 1.4 kg/kw. This latter estimate was used to calculate the reduction in payload due to power-conversion equipment in figure 1. An efficiency of 90 percent was assumed for this equipment.

Power losses and propellant loss in the thrustor may also seriously reduce the payload capacity. As shown in reference 10, the thrustor efficiency η is

$$\eta \equiv \frac{\frac{1}{2} F^2/\dot{m}_{tot}}{\mathcal{P}} \qquad (3)$$

If some of the propellant is not ionized and accelerated, the efficiency may be written as

$$\eta = \left(\frac{\dot{m}_+}{\dot{m}_{tot}}\right) \frac{F^2}{2\dot{m}_+ \mathcal{P}} \qquad (4)$$

where $\dot{m}_+$ is the propellant that is ionized and accelerated (for simplicity only singly charged propellant particles are considered here). A propellant utilization efficiency may be defined that accounts for the propellant loss:

$$\eta_U \equiv \frac{\dot{m}_+}{\dot{m}_{tot}} \qquad (5)$$

and a power efficiency may be defined that accounts for electric power loss:

$$\eta_P \equiv \frac{F^2}{2\dot{m}_+ \mathcal{P}} \qquad (6)$$

From these definitions the thrustor efficiency is

$$\eta = \eta_U \eta_P \qquad (7)$$

The efficiency of an existing Lewis electron-bombardment thrustor has been used to illustrate the effect of current thrustor inefficiencies on payload capacity in figure 1.

The mass of thrustors can also reduce payload capability. This mass is strongly dependent on specific impulse and durability requirements. The mass of existing thrustors is a substantial fraction of the payload mass, as illustrated in figure 1. The reduction in payload shown in

figure 1 is based on extrapolation of durability test data (to be discussed later) for the current Lewis electron-bombardment thrustor. The optimization procedure used is described in reference 10.

From figure 1, it is evident that existing thrustors would cause considerable loss in payload or trip time due to thrustor inefficiency, thrustor mass, and operation at constant specific impulse. Power-conversion systems, even of an advanced design, would also cause much payload loss. The net result of these losses is equivalent to an increase in overall specific weight from the assumed powerplant value 4 kg/kw to about 10 to 15 kg/kw. Further calculations (presented in ref. 10) show that existing thrustors would cause even greater relative loss in payload capacity for Mars round-trip vehicles. Although space flight is possible with existing thrustors, the potential gains in payload capacity warrant a critical examination of the various electrostatic thrustor-design concepts with regard to their possible improvement and ultimate performance.

ELECTROSTATIC THRUSTOR PRINCIPLES

In the electron-bombardment thrustor, propellant atoms or molecules are ionized by electron impact. A plasma results in the ionization chamber. The ions are extracted from the plasma by virtue of the electric field in the accelerator. Propellants of interest in present electron-bombardment thrustors are cesium, mercury, and heavy molecules (mass greater than 200 amu).

In the contact-ionization thrustor, atoms are ionized by surface contact of a low-ionization-potential atom on a high-work-function surface. The surface is hot so that the ions are evaporated, after which

they are accelerated by the electric field of the accelerator. The combination of most interest is cesium as the propellant and wolfram as the surface.

The colloidal-particle thrustor is still in a state of basic and applied research. There are a number of schemes for particle generation and charging, which will be discussed in later sections. Propellant mass-to-charge ratios of less than 100,000 amu per electronic charge are of interest.

All these thrustors produce thrust with the same basic principle, which is the acceleration of charged particles in an electric field, as indicated in figure 2. Electrons removed from the propellant particles are drawn from the high potential charging chamber, or ionizer, by the electric powerplant and are injected into the charged-particle exhaust. The charged particles merely fall through the potential difference to obtain the desired exhaust velocity.

It is essential that the charged-particle exhaust be neutralized, particularly since the accelerator is at or near space-charge-limited current density (refs. 17 and 18). This neutralization requires: (1) equal rates for the ejection of opposite charges (current neutralization) to avoid building up a large charge on the space vehicle, and (2) equal densities of opposite charges in the beam (charge neutralization) to avoid large space-charge effects within the beam. Early theoretical analyses predicted that beam neutralization would be a serious problem; however, early experimental operation in vacuum facilities indicated that the exhaust beams were in fact neutralized (ref. 19). In a series of

definitive experiments, Dr. J. M. Sellen showed that ion beams up to 10 ft in length could be neutralized under closely simulated free-space conditions (ref. 20). From these experiments, it appears that beam neutralization will not be a fundamental problem. To obtain absolute verification, beam neutralization will be tested in the SERT-1 space flights described in reference 21.

The remaining neutralization problem appears to be the development of durable neutralizers. The electron emitter should be only a few volts below the potential of the neutralized beam. Because of space-charge limitations on electron current, it is necessary to have a very short distance between the electron emitter and the ion beam if the electron emitter is to have a reasonably small size. If the edge of the ion beam were sharply defined, the neutralizer could simply be brought up close to the edge of the beam. Even if the ion optics were good enough to make a sharply defined beam edge, charge-exchange ions would probably make some sort of shadow shielding necessary for long-life neutralizers.

An estimated life of 25 hours was obtained for one of the shielded configurations investigated in reference 22. This short lifetime was probably the result of charge-exchange ions formed near the neutralizer. Since the potential difference between the neutralizer and the exhaust-beam plasma was over 50 volts for this configuration, these charge-exchange ions were sufficiently energetic to cause considerable sputtering erosion. A better shielded-neutralizer design with only a 10- to 20-volt potential difference between it and the beam should have no trouble reaching any desired lifetime. Since the neutralizer does not

appear to offer any major problems and since neutralization problems are substantially similar for all types of thrustors, they will not be considered further. It is true that a colloidal-particle thrustor may require a supply of protons rather than electrons, but such a neutralizer should still be a minor problem compared to the rest of the thrustor.

ELECTRON-BOMBARDMENT THRUSTOR

A typical electron-bombardment thrustor is shown in figure 3. Energetic electrons, contained by electric and magnetic fields, are used to ionize atoms in this thrustor. Production of ions by electron bombardment is not a new concept. But previous electron-bombardment ion sources that produced sufficient ion current to be of interest for electric propulsion (such as ref. 23) had current densities too high to be transmitted by practical accelerator systems. The contribution of references 24 and 25 was primarily an electron-bombardment ion source that matched the current-density requirements of a long-life electrostatic accelerator system operated in the specific impulse range of interest.

The performance of electron-bombardment thrustors obtained in the initial investigations showed substantial advantages as compared with other ion thrustors of that period (ref. 26). Because of these advantages, a sustained research program on this type of thrustor has been conducted at the NASA Lewis Research Center. More recently, contractual work with private industry has augmented the work at Lewis (refs. 27 to 29).

The propellant is vaporized and passes through the distributor into the ion chamber. In the ion chamber the propellant is bombarded

by electrons from the cathode. The collisions of electrons with the
propellant atoms are enhanced by an axial magnetic field, which prevents
the rapid escape of electrons to the anode. Escape of electrons to the
ends of the ion chamber is prevented by operating these ends at the same
potential as the cathode. Some of the propellant becomes ionized by the
bombardment of electrons, and some of these ions arrive at the screen
and are accelerated into the ion beam. (The ions that are not acceler-
ated into the ion beam recombine with electrons at the walls of the ion
chamber.) An electron source (not shown in fig. 3) then neutralizes
this ion beam.

The problem areas of this type of thrustor can be divided into
those of the ion chamber, the magnetic field, the cathode, and the ac-
celerator. These problem areas will be discussed in this order in the
following sections.

Ion Chamber

Following the initial investigations of references 24 and 25, an
extended investigation was conducted to determine optimum ion-chamber
geometry. This investigation is described in reference 30. The op-
timum of the cylindrical ion-chamber geometries investigated was a
length approximately equal to the diameter, and the anode length nearly
equal to ion-chamber length. Some optimization of distributor design
was found desirable for each combination of current density and specific
impulse. The ion chamber was otherwise found to be insensitive to small
changes in geometry, and after extended testing, the optimum geometry
did not differ greatly from the best geometry reported in reference 24.

The discharge power, approximately the cathode emission times the ion-chamber potential difference, is shown as an energy per beam ion in figure 4 for mercury propellant and a good geometry. Some development is required to obtain this level of performance, but it has been obtained many times - and frequently exceeded. In addition to changing the distributor, the accelerator geometry may also have to be changed, as discussed in the "Accelerator" section.

The standard operating condition for references 24, 25, and 30 was with a 50-volt potential difference between the anode and cathode in the ion chamber. With this potential difference, it was found, in reference 31, that 5 to 10 percent of the ions leaving the ion chamber were doubly ionized, which would correspond to a thrust loss of $1\frac{1}{2}$ to 3 percent and an efficiency loss twice as large. Dropping the ion-chamber potential difference to 30 volts had little effect on the discharge energy per beam ion, but the percent of doubly ionized ions was found to decrease to 2 to 5 percent. This reduction in potential difference also had the beneficial effect of reducing cathode sputtering.

Cesium has been investigated as a propellant for an electron-bombardment thrustor designed by Dr. R. C. Speiser (ref. 27). A photograph of this thrustor is shown in figure 5. The results indicate that a somewhat lower discharge energy per beam ion can be expected with cesium as the propellant (as indicated by the second curve in fig. 4). Even with the lower discharge power, though, the lower atomic weight of cesium (132.9 versus 200.6 for mercury) would result in lower thrustor efficiencies unless additional power savings were made elsewhere. As

will be discussed in the Cathode section, such additional power savings are possible.

Propellants with even heavier atomic weights than mercury would be desirable for improving both the efficiency and thrust density of an electron-bombardment thrustor at low specific impulses. Since prospective propellants do not exist as atomic species much heavier than mercury, heavy molecules appear to be the only practical substitute. An investigation of possible heavy-molecule propellants is being conducted at Lewis (ref. 32). Complete results have not yet been reported, but considerable experimental work has been completed. Preliminary analysis of the data indicates that molecules substantially heavier than mercury can be ionized and accelerated into a beam, but only for propellant utilizations less than 10 percent. The mean molecular weight is reduced due to fragmentation at higher utilizations. Further experiments are planned, but the simultaneous achievement of high utilization and high mean molecular weight does not appear likely.

Some improvement in ion-chamber performance might be obtained through ion-chamber accelerator interactions, as is discussed in the "Accelerator" section. It is felt, though, that near-optimum geometry has already been obtained for the ion chamber and that further improvements would be small and difficult to achieve.

No problems were encountered concerning durability in the ion chamber (with the exception of the cathode, which is treated in a separate section) even though material as thin as 0.2 or 0.3 mm was used for various parts.

Magnetic Field

The problem that has been associated with the magnetic field in the past has been a compromise between weight and power. Solenoidal windings on research thrustors, where weight is unimportant, can be quite heavy and have correspondingly low power losses. Such windings may weigh as much as 10 lb for a thrustor with a 10-cm-diameter beam, and have only a 50-watt power loss. On the other hand, a flight-type thrustor may have a field winding that weighs only 1 lb but have a power requirement of 200 watts.

A recent paper (ref. 33) indicates a solution to the power-weight problem. The permanent-magnet design investigated in reference 33 has a mild-steel distributor plate and screen with permanent magnets positioned between the two. A photograph of this thrustor is shown in figure 6. As shown in reference 30, ion-chamber performance is improved when the field strength at the screen is less than that at the distributor. The disparity in sizes of the two pole pieces (distributor and screen) shown in figure 6 is one means of obtaining this field strength difference.

Except that no field power was required, the permanent-magnet electron-bombardment thrustor operated in a normal manner. Extended operation and cycling conducted since reference 33 was published has resulted in no significant change in magnetic field strength. The only adverse results are a lack of operating flexibility (which is of interest mainly in research) and decreased thermal-structural stability of the mild-steel screen as compared to the molybdenum screen it replaced. More

careful design for thermal-expansion effects should solve this latter problem.

One of the most important virtues of the permanent-magnet design of reference 33 is its low weight. The total weight of the permanent-magnet thrustor is 3 lb, which is almost exactly the weight of a flight-type thrustor of the same size (10-cm-diameter beam) that employed a high-loss, low-weight solenoidal winding.

Cathode

Both power and lifetime problems are associated with the cathode. The early electron-bombardment thrustor experiments at the Lewis laboratory were conducted with tantalum, and occasionally wolfram, cathodes. Although pure tantalum has severe power and durability problems, it is very easy to use and gives reproducible results. A desired lifetime with tantalum is achieved simply by supplying sufficient cathode material to offset sublimation and erosion. From tests with tantalum strips at Lewis (ref. 34), it appears possible to use tantalum for attitude-control thrustors where the actual operating time may only be 1000 to 2000 hr, and efficiency is not of primary importance. For main propulsion systems, with anticipated lifetimes of perhaps 10,000 hr, tantalum cathodes are out of the question. Wolfram, with electron-emission characteristics similar to tantalum, would also be unacceptable.

A more promising type of cathode uses alkaline-earth carbonates in a composite structure with nickel or some other relatively inert metal. The metal provides a structural matrix to hold more of the emitter material than could be applied with just a coating on the outer surface. A

nickel-matrix cathode described in reference 28 was operated in an electron-bombardment thrustor designed at Ion Physics Corporation (fig. 7) for periods up to 300 hr. Investigations have been conducted at Lewis with another type of metal-matrix cathode. One test at Lewis in a simulated thrustor (a complete thrustor except for the accelerator) had a duration of more than 1600 hr. The heater power increased with time, going from about 15 to 30 watts per emitted ampere at the end of 1600 hr. The performance obtained to date indicates that good efficiency for a 10,000-hr life may be possible with this type of cathode.

A final type of cathode to be considered is the autocathode being developed by Electro-Optical Systems in conjunction with the electron-bombardment thrustor of their design (fig. 5) reported in reference 27. Use of cesium propellant to provide a low work function emitter surface and ion bombardment for heating it results in a long-life cathode that requires no heating power. The ion-chamber potential difference with cesium as the propellant can be sufficiently low so that cathode sputtering is not a problem, and the temperature of a cesium-coated cathode can be so low that sublimation of the base metal should be negligible. Thus, there should be no major obstacle to the attainment of a 10,000-hr lifetime, or even longer, with this type of cathode. The major shortcoming is the increased charge-exchange cross section of cesium, which serves to limit the thrust-to-area ratio of the accelerator.

The ion chamber, the magnetic field, and the cathode, just discussed, are the major loss sources in a well-designed electron-bombardment thrustor. A good estimate of the performance that can be expected with

mercury as the propellant is obtained by selecting an electron emitter loss of 20 watts per emitted ampere, a 30-volt ion-chamber discharge, and the discharge losses quoted in the Ion Chamber section. An additional 1-percent jet-thrust loss may be assumed for impingement and off-axis velocity effects. The performance calculated with these assumptions was presented in reference 35, and is shown in figure 8. A trade-off can be made between ion-chamber and propellant-utilization losses. The optimum utilization (for efficiency) is also shown in figure 8. Although a minimum power-to-thrust ratio of about 100 kw/lb is shown in figure 8, operation below about 4000 sec is difficult because of accelerator current-density limitations. A power-to-thrust ratio of about 150 kw/lb would therefore be a more realistic lower limit. Similar calculations were made for cesium as the propellant. The assumptions were the same except that the lower discharge losses of cesium were used, and a 20-volt discharge was assumed. A small cathode power loss of 5 watts per emitted ampere was assumed so that better control of the discharge could be obtained than with an autocathode. The optimum efficiency obtained with cesium was about 1 percent higher than that shown in figure 8. The optimum utilization was also increased 1 to 2 percent over that of figure 8. Although the curves of figure 8 are calculated, experimental values within a few percent of the maximum efficiency curve have been obtained over a wide range of specific impulse.

Accelerator

The problem posed by the accelerator is primarily one of durability. A thorough study of accelerator configurations for the electron-

bombardment thrustor was conducted at Lewis and is presented in refer-
ences 36 and 37. As shown in reference 36, operation well below space-
charge limitations with a carefully aligned accelerator system can result
in impingement currents approaching that from charge exchange alone.
Later tests at Lewis (ref. 38) have verified this conclusion. (With
mercury as the propellant, the ion-impingement and accelerator-drain
current are substantially equal. The measurement of ion impingement
with mercury is therefore much simpler than with cesium.)

As shown in reference 38, the accelerating system of existing
thrustors with 10-cm-diameter beams should last 10.000 hr at a specific
impulse of 4000 sec and a propellant utilization of 76 percent if the
current of mercury ions does not exceed about 0.13 amp. This lifetime
corresponds to a total ion impingement of 3.3 amp-hr, which is suffi-
cient to erode through the thinnest sections of the accelerator. The
variation of lifetime $\mathcal{L}$ with ion-beam current and propellant utiliza-
tion is of the form

$$\mathcal{L} \propto \frac{\eta_U}{1 - \eta_U} \frac{1}{J_B^2} \tag{8}$$

when charge exchange is assumed to be the primary cause of accelerator
impingement. The effect of specific impulse on lifetime is also of in-
terest. However, since different combinations of net accelerating po-
tential difference Φ_{net} and propellant utilization can yield the same
specific impulse, the ion energy (and hence sputtering damage) therefore
does not have a unique relation with specific impulse. A working rela-
tion for the effect of specific impulse may be obtained by assuming

utilizations near the optimum for efficiency, as shown in figure 8. The lifetime proportionality thereby obtained is

$$\mathcal{L} \propto \frac{\eta_U}{1 - \eta_U} \frac{1}{J_B^2} \left(\frac{4000}{I}\right)^{1.13} \qquad (9)$$

Using the lifetime data at 4000 sec from reference 38 for a 10-cm beam thrustor yields a constant of proportionality. The maximum ion current for this size thrustor is thus:

$$J_B = \left[\frac{2.23}{\mathcal{L}} \left(\frac{\eta_U}{1 - \eta_U}\right) \left(\frac{4000}{I}\right)^{1.13}\right]^{1/2} \qquad (10)$$

with $\mathcal{L}$ the lifetime in days. This equation, together with an actual single module weight of 3 lb, was used to calculate weight figures for an electron-bombardment thrustor shown in figure 9. Figures 8 and 9 were used for the calculations of figure 1. Any desired lifetime can be obtained simply by reducing the ion-beam current to a small enough value. The efficiency of an electron-bombardment thrustor, unlike that of a contact-ionization thrustor, is substantially independent of current density. The only adverse effect of lowering the ion current density is the increased size, and hence weight, of the thrustors.

The effect on the accelerator lifetime of changing the propellant to cesium can be estimated by comparing charge-exchange cross sections and atom-ion sputtering ratios for cesium and mercury (refs. 38 to 40). The charge-exchange cross section for cesium is two to three times as large as that for mercury. The effect of the larger charge-exchange cross section for cesium, though, is almost balanced by a reduced sputtering (using molybdenum for both). If it is assumed that these two

factors balance, the only effect left would be that of charge-to-mass
ratio and spacing of the accelerator. Since the acceleration voltage
for a given specific impulse will be less with cesium, closer accelerator
spacings might be expected with cesium, which would lead to reduced
charge-exchange impingement. However, the thrustor weight is greatest
at low specific impulses, where the same minimum accelerator spacing
(determined by fabrication and structural stability considerations) will
probably be used for both cesium and mercury. Thus, although the use of
cesium gives the best prospects of a long-life cathode, it will probably
cause substantial increases in thrustor weight at low specific impulses.
For the same accelerator spacing, the thrust per unit area with cesium
would only be about two-thirds that with mercury.

The final topic for the accelerator section concerns the interaction
with the ion chamber. The data for the various accelerator configurations
investigated in reference 36 show substantial effects of accelerator con-
figuration on ion-chamber performance. In general, increasing the per-
centage of open area in the screens, reducing the screen thickness, and
increasing the accelerating potential difference resulted in lower ion-
chamber discharge power loss. One aspect is certainly the loss of ions
due to collision on the screen. Changing the variables in the direction
indicated will tend to reduce these collisions. It is difficult, though,
to explain all of the observed interactions in terms of ion-screen colli-
sions. The electric field from the accelerator system apparently can in-
fluence ion motion in a substantial portion of the ion chamber, far more,
for example, than would be indicated by a calculation of Debye shielding

distance (less than 0.1 mm). In any event, the accelerator configuration can have a substantial effect on ion-chamber performance. This effect should be considered when trying to optimize performance.

As may be surmised from the preceding discussion, several areas of research on the electron-bombardment thrustor appear to be reaching completion. The ion-chamber configuration, magnetic-field design, and the accelerator structure all fall into this category. A possible exception might be an attempt to produce more uniform current density, which would permit considerably greater power densities for the same lifetime.

The cathode is probably the most important remaining component research area. The cesium autocathode described in reference 27 is one promising solution. As was pointed out, however, the use of cesium places more severe limits on the thrust-to-area ratio at low impulse than does mercury. This effect alone is sufficient reason to continue research on alkaline-earth carbonate cathodes, particularly since very substantial lifetimes have already been obtained. Another reason for continuing research on the alkaline-earth carbonate cathode is the possible use of other propellants to obtain variable specific impulse operation.

CONTACT-IONIZATION THRUSTORS

The basic concept of the contact-ionization electrostatic thrustor was presented by Dr. E. Stuhlinger in 1954 (refs. 41 and 42). Since the beginning of active experimental work on electric thrustors in 1957-58, the major share of research and development has been devoted to the contact-ionization thrustor.

The distinguishing feature of this thrustor is the method of ionization of propellant atoms. Stuhlinger noted that alkali metal atoms such as cesium could be ionized with high probability on surfaces with high work functions such as wolfram and then could be accelerated with an electrostatic field, as indicated in figure 10. The early work on the contact-ionization process by Irving Langmuir, Becker, and others showed that the cesium-wolfram system provided ionization probabilities as high as 99 percent. In order to preserve the high work function, however, it was necessary to allow only a small fraction of a cesium monolayer on the wolfram surface. This was accomplished by maintaining the wolfram surface at a high temperature (1300° to 1500° K).

The high temperature causes a considerable thermal-radiation loss, thereby reducing the thrustor efficiency (by increasing the power $\mathscr{P}$) as shown by equation (3). To obtain a reasonable efficiency, a high ion-beam power per unit area must be attained. Ion-beam power density may be limited by minimum practical accel distances. For a fixed accel distance, cesium provides a higher exhaust-beam power density than the other alkali metal atoms by virtue of its highest mass.

For the reasons of highest ionization probability and highest beam power density, the cesium-wolfram system has been generally accepted as the best for the contact-ionization thrustor. From such optimistic beginnings, contact-ionization thrustors have progressed through much research and development and stand today as nearly flight-worthy devices.

One type of contact-ionization thrustor is under development at Electro-Optical Systems. The progress and performance of this thrustor

are described in references 43 to 48, and a photograph of one of the design versions is shown in figure 11. Another type of contact-ionization thrustor is under development at Hughes Research Laboratory. The progress and performance of this thrustor are described in references 49 to 53, and a photograph of one of the design versions is shown in figure 12.

Both of these thrustors are based on common fundamentals, so they will be discussed concurrently. Both have porous wolfram ionizers. By virtue of its own vapor pressure, cesium diffuses through the pores of the ionizer and is ionized by contact on the "downstream" face of the ionizer. The cesium ions are then accelerated by the accelerator electrodes. The cesium ions are singly charged, so their final speed is uniform.

The major power loss in these thrustors is due to thermal radiation from the ionizer. Conduction heat loss has been minimized, and the "upstream" side of the ionizer and propellant-feed manifolds are well insulated to minimize thermal-radiation loss. The accel length has been made as short as presently possible and is only a few millimeters in both thrustor concepts.

As shown in figures 11 and 12, the EOS thrustor consists of an array of ionizer "buttons" and circular electrode apertures, while the Hughes thrustor consists of concentric "annular" ionizers and exhaust apertures. Both thrustors have concave ionizer surfaces but different electrode shapes. The neutralizer designs are also different.

Ion Optics

Inasmuch as the ions come from a physical surface in the contact-ionization thrustor (as opposed to a diffuse plasma in the electron-bombardment thrustor), the boundary values for the acceleration process can be well defined. A variety of theoretical methods of predicting ion trajectories therefore can and have been used. Analytic solutions are summarized in reference 54, while numerical methods of solution are given in references 55 and 56. An electrolytic-tank analog computer has been a standard design tool at Hughes. The rubber-sheet analog has also been used various places but is limited in usefulness due to the impracticality of space-charge simulation.

Theoretical solutions to the acceleration process are of greater importance for the contact-ionization thrustor, than for the electron-bombardment thrustor. Direct impingement of primary ions is masked not only by impingement of charge-exchange ions but by electron emission (both secondary and thermionic) from the accel electrode. Drain currents from the accel electrode may be as high as 15 percent of the ion-beam current at ion current densities of 250 amp/sq m (ref. 57). A recent theoretical analysis (ref. 58) shows that thermionic electron-emission currents from the accel electrode may be very high fractions of the cesium ion current. Neutral cesium atoms from the ionizer can form a layer on the accel electrode, thereby producing a low work function surface and resulting in high electron-emission currents. The analysis predicts that either cooling or heating the accel electrode a few hundred degrees Kelvin will reduce the electron-emission current to a negligible level.

Both the EOS and Hughes thrustors are believed to have satisfactory ion optics. In both thrustors, the ion beam is slightly "overfocused" so that the edge of the beam is a finite distance from the accel and decel electrodes. This separation distance eases design and fabrication tolerances and reduces the effect of ion thermal velocities to a negligible level.

Computer solutions for space-charge-flow geometries such as the EOS and Hughes thrustors show that a considerable variation of ion current density may occur across the ionizer surface (ref. 57) without excessive impingement. Nonuniform current density, though, may have other consequences, to be discussed later.

Charge Exchange

Although the cesium-wolfram system has a very low emission rate of neutral cesium atoms under ideal conditions, this emission is not negligible. Optimization of efficiency requires that maximum current and power densities be used. The optimum is, of course, the highest current density that is consistent with lifetime requirements. As was mentioned in the preceding section, measurement of ion impingement is complicated by electron emission from the accelerator electrode. The erosion effects of charge-exchange ions must therefore be determined either from actual lifetime tests or from theoretical studies.

A theoretical study at Hughes with the electrolytic-tank analog computer showed that charge exchange in only a portion of the region near the electrodes contributes to charge-exchange impingement (ref. 29). The region that produces charge-exchange interception for a particular electrode configuration is shown in figure 13.

The durability of the EOS and Hughes thrustors has not been fully established either on a theoretical or an experimental basis. It is nevertheless of interest to estimate the durability of their electrodes with the data obtained for the bombardment thrustor in reference 38. If it is assumed that equal amounts of accelerator electrode material erosion are allowable in cesium and mercury thrustors, that the volume of the charge-exchange region and the accelerator designs are the same, and that the charge-exchange cross sections are $\sigma_{Hg} = 6 \times 10^{-15}$ sq cm (ref. 38) and $\sigma_{Cs} = 2 \times 10^{-14}$ sq cm (ref. 39), then the ratio of allowable current densities is:

$$\left(\frac{j_{Cs}}{j_{Hg}}\right)_{\Phi} = 0.55 \left(\frac{Y_{Hg}}{Y_{Cs}}\right)^{0.5} \left(\frac{1 - \eta_U}{\eta_U}\right)_{Hg}^{0.5} \left(\frac{\eta_U}{1 - \eta_U}\right)_{Cs}^{0.5} \tag{11}$$

From reference 38, the sputtering yield is $Y_{Hg} = 1.5$ atoms per ion for 5000 ev Hg^+ incident on molybdenum. The EOS thrustor has copper accel electrodes, so that sputtered atoms of copper cannot contaminate the ionizer (the melting point of copper is less than the ionizer operating temperature). From reference 39, $Y_{Cs} = 6$ atoms per ion for 5000 ev Cs^+ incident on copper. For the same accel potential Φ_A and assuming that Y_{Hg} and Y_{Cs} are both proportional to $\Phi_A^{0.7}$,

$$\left(\frac{j_{Cs}}{j_{Hg}}\right)_{\Phi} = 0.27 \left(\frac{1 - \eta_U}{\eta_U}\right)^{0.5} \left(\frac{\eta_U}{1 - \eta_U}\right)_{Cs}^{0.5} \tag{12}$$

With this expression, it is possible to estimate the comparative performance of the contact-ionization thrustor with that of the electron-bombardment thrustor previously described. The durability of the

electron-bombardment thrustor is for the overall thrustor module and is limited by the current density at the center of the accel electrode plate. This current density is about three times the average current density of the module. By applying this correction, it is possible to make a rough estimate of the allowable exhaust-jet power density of a comparable contact-ionization thrustor. The results of this estimate are shown in figure 14 for an accel electrode durability of 400 days. If a material with a low sputtering coefficient could be used for the accel electrode in place of copper in the contact-ionization thrustor, it might be possible to double the power densities shown in figure 14. The low power densities shown in figure 14 could have a serious adverse effect on thrustor size and specific mass. A similar consequence exists with regard to thrustor efficiency, which will be discussed in the next section.

It should be noted that the calculations presented in figure 14 are subject to the accuracy of the assumptions. In charge-exchange ion erosion of the accel electrode, the allowable current density is inversely proportional to the square root of the charge-exchange cross section, charge-exchange region volume, and sputtering yield. This relation tends to reduce the sensitivity of the value of current density to errors in the other parameters. For this reason, the estimate shown in figure 14 may be used with a fair confidence.

Porous Ionizer

From the preceding brief discussion and approximate calculations regarding charge exchange, it is clear that low neutral-atom concentration is essential for contact-ionization thrustors. Since the ionizer

is responsible for admitting neutral cesium atoms, it is appropriate to examine the status of this component in detail.

Because of the charge-exchange problem, the porous ionizer has been accepted as being superior to solid ionizers (with a reverse flow of fresh neutral atoms passing through the ion beam). In porous ionizers, the cesium vapor flows through the ionizer pores by both Knudsen flow and surface diffusion. If the flow rate due to surface diffusion is greater than that due to Knudsen flow near the pore exit, the predominant fraction of the cesium will flow onto the downstream face of the ionizer, as indicated in figure 15. Theoretical analyses of this model of flow and ionization have indicated the need for submicron pore diameters at high ion current densities (refs. 59 to 61). Experimental data on the neutral-atom efflux from small samples (5 mm diameter) show that neutral efflux increases as ion current is increased (refs. 62 to 66). Typical data are shown in figure 16, taken from reference 64, for a pore size of about 2 microns and a pore density of 10^6 cm^{-2} with various porous materials. Porous ionizers with these characteristics are commercially available.

Experimental data recently reported in reference 65 confirm the need for small pore size. Wolfram ionizers made from spherical powder, and others made from wire bundles, were compared with commercial wolfram samples having a 2-micron pore diameter and 2×10^6 pores per square centimeter. The neutral atom efflux from these ionizers is shown in figure 17. It is evident that the spherical-powder wolfram ionizers provide a lower neutral-atom fraction.

To obtain satisfactorily low neutral-atom flux, the pore size must be smaller than presently obtainable, and the pore density (number per unit area) must be high, for instance, greater than 3×10^6 cm^{-2} (ref. 64). The use of small diameter wolfram powder would presumably provide these requirements; however, it appears that with small powder diameters, the porous ionizers continue to sinter at the ionizer operating temperature. This sintering fills up the pores and increases the density of the ionizer, resulting in increased neutral-atom efflux that eventually result in cracking due to reduction in volume. At Hughes, several porous-wolfram ionizers with 2- to 4-micron pores have been operated for 11 months at 1440° K (ref. 64). The 4-micron pore-size ionizers appear to have retained stability over this time, but the 2-micron pore-size ionizers have suffered substantial increases in flow transmission coefficient. It is possible that this increased flow may indicate the presence of microcracks caused by reduction in volume due to sintering. Thus, small powder diameter wolfram ionizers of the type necessary for low neutral-atom effluxes may sinter shut or crack during the lifetimes required for space flight.

In addition to the effect on long-term ionizer sintering, the ionizer temperature is also of great importance to thrustor efficiency, because thermal radiation from the ionizer constitutes the major power loss. In early work on contact ionization, it was found that below a certain critical temperature mostly neutral atoms are evaporated from the surface, while above this temperature mostly ions are emitted. A similar critical temperature is found for porous emitters, although the

ion-atom emission does not change as sharply as for solid surfaces. The effect of ionizer temperature on ion current density and neutral-atom fraction is exhibited by typical data from reference 65 shown in figure 18. Neutral-atom efflux minimizes at about 1460° K (this is the neutral-fraction critical temperature), while the ion critical temperature occurs at about 1360° K in figure 18. Operation at minimal neutral-atom flux would increase the thermal-radiation loss by 37 percent in this case. The data in reference 64 suggests that smaller pore size and increased pore density could reduce the critical temperatures for ion current and neutral-atom fraction. This is supported by the theoretical analyses of references 59 to 61.

As mentioned in the section Ion Optics, particular thrustor designs may have a nonuniform current density across the ionizer surface. It is evident that the ionizer must be operated at a temperature high enough to accommodate the highest local current density. Typical neutral-fraction critical temperatures given in reference 65 for spherical-powder wolfram ionizers are shown in figure 19. If the average current density were 60 amp/sq m and a peak existed at 180 amp/sq m, the increase in ionizer temperature required to prevent high neutral-atom efflux from the high current spot would result in a 25-percent increase in thermal-radiation loss.

With the equations presented in the Charge Exchange section, it is possible to estimate the maximum thrustor efficiency on the basis of the best existing porous-wolfram characteristics. The spherical powder data from figure 17 were used. The emittance of porous ionizers may be subject

to surface conditions (ref. 64); so an average value of 0.5 was assumed herein. The heat loss is assumed to be only the thermal radiation from the downstream face of the ionizer. With these assumptions, the estimated maximum efficiency is shown in figure 20 together with the present efficiency of the electron-bombardment thrustor. Figure 20 illustrates the comparatively insensitive nature of this estimate to small errors, with a 3 to 1 difference in accelerator spacing resulting in an 11-percent efficiency change, or less. Figure 20 also illustrates the serious shortcomings of present porous-wolfram technology. Without drastic improvements in this technology, present electron-bombardment efficiencies cannot be equaled with long-life contact-ionization thrustors.

A similar estimate of exhaust-jet power density is shown in figure 21, which shows that contact-ionization thrustors are about the same size as electron-bombardment thrustors. However, contact-ionization thrustors probably require heavier construction than electron-bombardment thrustors and will not have lighter weights than those shown in figure 9.

The estimates of contact-ionization thrustor performance made herein are based on the use of a single set of accel electrodes. It is evident that if the accel electrodes could be replaced en route with reliable, lightweight mechanisms, then the allowable current density would be increased and higher performance would be possible.

The present efficiencies of EOS and Hughes thrustors (reported in ref. 67) are shown in figure 22. These efficiencies are maxima and are not necessarily compatible with durability requirements of interplanetary missions.

The neutral cesium atom efflux from porous-wolfram ionizers can be reduced if uniform submicron pore sizes and high pore densities (number per unit area) can be obtained. At the same time, sintering at ionizer operating temperatures must be slow enough so that the ionizer has a durability of at least 400 days. This ionizer problem has been recognized for a number of years, and many man-years of applied research have been devoted to ionizer improvement. In spite of this effort, satisfactory porous-wolfram ionizers have not yet been developed.

A number of possible research avenues are discussed in reference 68. These avenues are, in one form or another, presently under investigation in a number of laboratories.

Other geometries also offer some hope of improved performance for contact-ionization thrustors. Examination of figure 13 shows that charge-exchange impingement results primarily from charge-exchange processes near the accelerator, with those occurring near the ionizer being relatively unimportant. A divergent-flow thrustor, such as described in reference 69 and shown in figure 23 would have a high current density at the ionizer to decrease the heat loss, but a low current density near the accelerator, where most of the erosion effects originate. Calculations for a divergent-flow thrustor (with an area ratio of 2 between the ionizer and the beam at the accelerator aperture) indicate that efficiencies slightly better than those of present electron-bombardment thrustors might be achieved with present porous-wolfram technology.

Perhaps the lower neutral fractions and heat losses of solid-wolfram ionizers would even justify a return to the reverse-feed concept

described in references 70 to 72. If the neutral cesium were introduced close to the ionizer, as indicated in figure 24, the charge exchange would be substantially restricted to the "safe" region near the ionizer.

COLLOIDAL-PARTICLE THRUSTORS

Complete colloidal-particle thrustors do not exist at present. Devices have been operated in which colloidal particles are generated, charged, and accelerated; but these are only preliminary experiments and do not qualify as thrustors. The purpose of this section is to review and evaluate experimental work on potential colloidal-particle thrustor components.

The motivation for colloidal-particle research is similar to that for heavy molecules. By increasing the particle mass, the ratio of kinetic energy to charging energy should increase at any given exhaust velocity, thus raising the efficiency. This increase in efficiency is most needed in the lower range of specific impulses, so the generation of particles should be examined with a view to their use at these lower values. A number of particle generation schemes are presently being investigated. The minimum mean mass-to-charge ratio m/q that has been obtained experimentally with each of these methods is as follows:

Method	Minimum mean m/q, amu/Ze	Reference
Ion nucleation	1,400,000	73
Preformed (agglomerated) solid	950,000	74
Liquid drops from sprays	480,000	75,76
	14,000,000	77,78
Surface condensation	700,000	79
Vapor condensation	100,000	80,81

If a specific impulse of 5000 sec with a net accelerating potential difference less than 100 kv is considered, then the maximum usable m/q should be about 8000 amu/Ze. Even if the potential difference were raised to 10^6 volts, the maximum usable m/q would be below the values shown in the preceding table. Although work in this field has been going on for several years, the total research effort has been small.

Research is continuing on each of the above methods in an effort to provide the proper m/q range with good utilization efficiency.

Ion Nucleation

In the ion-nucleation method (ref. 73) a supersaturated vapor stream is partly ionized. The ions are intended to be condensation nuclei. By applying a retarding electric field, the nuclei are slowed down to provide enough time for particle growth. Charged particles with a large enough m/q would pass over the retarding potential difference, so that a supply of particles with uniform m/q would result. This method is still in the basic research stage.

Preformed Particles

Preformed solid particles with a mean size of 70 Å have been gravity fed through ducts to an electron-bombardment ionization chamber, ionized,

accelerated, and analyzed for charge/mass distribution (ref. 74). The particles were initially agglomerated and remain partly agglomerated through the charging process. However, the mass/charge ratio was only about a decade too high, so this experiment provides some evidence that the use of preformed solid particles might be possible.

Electric Spraying

A major share of the colloidal-particle-thrustor research has been devoted to particle generation and simultaneous charging of electrically sprayed liquid droplets. The drops are formed and charged at sharp hollow needle points (refs. 75 to 78) or at a sharp edge of a spinning cup (ref. 82) with a high electric field at the point or edge. Drop formation occurs by a combination of fluid instability and dielectro-phoresis (refs. 75 and 76). Charging occurs at the instant of separation from the tip by charge transfer.

The electric field strength must be high at the tip in order to obtain small drop sizes. If the field strength is too high, a glow discharge occurs that generates a large ion current. This ion current may cause a serious power loss in the accelerator. Recent experiments have shown that the electric spraying process may be sporadic (ref. 77). At first, the liquid tip is sharp, and small size charged drops are emitted. Then the liquid tip builds up and a very large charged drop is emitted accompanied by many ions. These sequences are sporadically repetitive. These data also show a very wide range of m/q.

The high-speed photomicrographic data of reference 77 indicate that if the liquid is conducting, the electric field penetrates the bulging

liquid drop at the tip preventing the formation of small drops. If the liquid is nonconducting, the high field strength is preserved, but a finite time is required to accumulate a charge in the "liquid tip". This low rate of charge accumulation limits the mass flow rate of liquid from each hollow needle. For example, a maximum current of 1 micro-ampere per needle is quoted in reference 75. If the net accelerating voltage were 10^6 volts, there would be 1 watt of thrustor exhaust power per needle. From the preceding sections it is evident that an exhaust power density of 100 kw/sq m is required in order to be comparable in size with the existing electron-bombardment thrustor at 5000 sec. At an exhaust power density of 100 kw/sq m, 10^5 needles would be required per square meter. The needle spacing would be 3 mm. It seems reasonable to expect that such a needle density would lower the electric field strength at each needle tip, perhaps below that required for electric spraying.

The charge-accumulation limit also appears pertinent to the surface-condensation scheme. In fact, the literature does not contain even ap-proximate analyses to demonstrate that the electric-spraying or surface-condensation schemes might be useful in real electrostatic thrustors.

Vapor Condensation

To date, the vapor-condensation method has not only produced values of m/q approaching the range of interest for propulsion (ref. 80) but has also been incorporated in a laboratory device that has produced a substantial thrust (ref. 81). In this method of particle generation, a supersaturated vapor enters a condensation shock wave where particle

nucleation occurs. Subsequent growth is controlled by the flow conditions. The colloidal particles are then charged by electron attachment in a glow discharge. Particle size distributions have been measured for a number of propellants such as $AlCl_3$, $HgCl_2$, and $HgCl$. Ion currents have not been observed. The fraction of total propellant that is converted into colloidal particles has yet to be determined.

The vapor-condensation method (refs. 80 and 81) is being investigated at Lewis in apparatus resembling a real thrustor. The past experiments have been made with a 50,000-volt power supply, but a 150,000-volt facility is now available, and a 400,000-volt facility is under construction. With such high-voltage power available, a greatly improved evaluation of this thrustor concept will be possible.

Quadrupole and monopole massenfilters (mass spectrometers) are being developed at Lewis for measurement of particle mass/charge in the exhaust beam from experimental thrustors. With measurements of particle mass/charge, thrust, beam current, particle size, and total propellant mass flow rate, it is expected that an accurate determination of propellant utilization can be made.

Fundamental studies of particle nucleation and growth are being made at Lewis. It is hoped that such studies will aid in the design of particle generator nozzles that will provide particles with a mass of less than 100,000 amu and with the narrow size distribution, which is necessary for good accelerator efficiency. In addition to the electron-attachment method of particle charging, several other methods are under investigation, which include electron bombardment, field emission, and photoionization.

CONCLUDING REMARKS

With the exception of the cathode, the electron-bombardment thrustor is capable of durabilities required for interplanetary round-trip missions. Experimental data from recent cathode tests indicate that alkaline-earth carbonate coatings may provide adequate durability at acceptable heater-power levels. It is also expected that the autocathode version of the electron-bombardment thrustor will have adequate durability. It is difficult to foresee any substantial improvement in the efficiency of the electron-bombardment thrustor. Although serious payload losses would be incurred with the electron-bombardment thrustor, it could be used for most electric-propulsion missions in its present form.

The ionizer in the contact-ionization thrustor is not adequate at present because of the inability to produce porous wolfram with sufficiently low neutral-atom loss and simultaneously to prevent unacceptable in-flight-sintering rates. Because of the high neutral-atom loss from porous wolfram ionizers, charge-exchange ion erosion of electrodes places a severe limit on contact-ionization thrustor efficiency, particularly in the lower range of specific impulse. The problems of porous wolfram ionizers - unless modified by substantial improvements in technology - are formidable enough to prevent the use of contact-ionization thrustors for primary propulsion.

Colloidal-particle thrustors do not exist at present. With the exception of the vapor-condensation method, existing methods of colloidal-particle generation produce particles with much too high a mass/charge ratio. At present, the vapor-condensation method would require accelerator voltages of 400,000 volts to obtain a specific impulse of 3000 sec,

which is near the lowest value of interest. Not enough is known at present to predict accurately the ultimate performance of the colloidal-particle thrustor.

Comparisons between electrostatic, electrothermal, and electromagnetic (plasma) thrustors have been avoided. Mission analyses (such as in ref. 10) show that the specific impulse of electrothermal thrustors is well below the range of interest for interplanetary missions. Existing plasma thrustors have unacceptably low efficiencies, and there is no concrete evidence at present on which to base estimates of future performance.

The development of moderately efficient thrustors, with excellent prospects of reaching desired lifetimes with further work, has served to highlight the shortcomings of electric propulsion as a system. The need for efficient, lightweight, reliable electric power sources and power-conversion equipment is particularly obvious.

REFERENCES

1. Evvard, J. C.: How Much Future for Electric Propulsion? Astronautics and Aerospace Engineering. August 1963.

2. Moeckel, W. E.: Electric Propulsion Systems for Mars Missions. Paper presented at Symposium on Exploration of Mars, Denver, Colorado, June 6-7, 1963.

3. Schipper, L., Siegler, R. S., and Zwick, E. B.: Advanced 1-Megawatt Space Power Plant Study. AIAA Paper No. 63-270, 1963.

4. Bernatowicz, D. T.: Thermionic Converters in a Large Nuclear Electric Powerplant in Space. ARS Journal, August 1962.

5. Elliot, D. G.: A Two-Fluid Magnetohydrodynamic Cycle for Nuclear-Electric Power Conversion. NASA JPL Technical Report 32-116, 1962. Also in ARS Journal, June 1962.

6. Beam, B. H.: An Exploratory Study of Thermoelectrostatic Power Generation for Space Flight Applications. NASA TN D-336, 1960.

7. Cox, A. L.: Colloidal Electrohydrodynamic Energy Converter. ARS Paper No. 2559-62, 1962.

8. Englert, Gerald W.: Study of Thermonuclear Propulsion Using Superconducting Magnets. Paper presented at Third Annual Conference on Engineering Magnetohydrodynamics, Rochester, N. Y., March 1962.

9. Mickelsen, W. R., and Low, C. A., Jr.: Potentialities of the Radio-isotope Electrostatic Propulsion System. AIAA Paper No. 63048A, 1963. Also in Astronautics and Aerospace Engineering, October 1963.

10. Mickelsen, W. R., and Kaufman, H. R.: Status of Electrostatic Thrustors for Space Propulsion. Proposed NASA TN.

11. Irving, J. H., and Blum, E. K.: Comparative Performance of Ballistic and Low-Thrust Vehicles for Flight to Mars. Vistas in Astronautics, vol. II, Pergamon Press, 1959.

12. Melbourne, W. G.: Interplanetary Trajectories and Payload Capabilities of Advanced Propulsion Vehicles. NASA JPL Technical Report No. 32-68, March 1961.

13. Sauer, C. G., Jr., and Melbourne, W. G.: Optimum Earth-to-Mars Roundtrip Trajectories Utilizing a Low-Thrust Power-Limited Propulsion System. Paper presented at Ninth Annual Meeting American Astronautical Society, Los Angeles, California, January 1963.

14. MacKay, J. S.: Unpublished Analyses. NASA Lewis Research Center, Cleveland, Ohio.

*15. Space Electric Power Systems Study. Fourth Quarter Progress Report, NASA Contract NAS5-1234. Aerospace Electrical Division, Westinghouse Electric Corp., Lima, Ohio, November 1962.

16. Corcoran, C. S., Jr.: Unpublished Analysis. NASA Lewis Research Center, 1963.

17. Kaufman, H. R.: One-Dimensional Analysis of Ion Rockets. NASA TN D-261, 1960.

18. Mirels, H., and Rosenbaum, B. M.: Analysis of One-Dimensional Ion Rocket with Grid Neutralization. NASA TN D-266, 1960.

19. Kaufman, H. R.: The Neutralization of Ion-Rocket Beams. NASA TN D-1055, 1961.

20. Sellen, J. M., and Kemp, R. F.: Cesium Ion Beam Neutralization in Vehicular Simulation. ARS Paper No. 61-84-1778, 1961.

21. Childs, J. H., and Cybulski, R. J.:   Flight Tests and Early Missions for Electric Propulsion Systems.   ARS Paper No. 2653-62, 1962.

22. Kemp, R. F., Sellen, J. M., and Pawlik, E. V.:   Neutralizer Tests on a Flight-Model Electron-Bombardment Ion Thrustor.   NASA TN D-1733, 1963.

23. Von Ardenne, Manfred: New Developments in Applied Ion and Nuclear Physics.   AERE Lib. Trans. 758, 1957.

24. Kaufman, Harold R., and Reader, Paul D.:   Experimental Performance of Ion Rockets Employing Electron-Bombardment Ion Sources.   ARS paper 1374-60, 1960.

25. Kaufman, H. R.:   An Ion Rocket with an Electron-Bombardment Ion Source.   NASA TN D-585, 1961.

26. Langmuir, David B., ed.:   Electrostatic Propulsion.   Vol. 5 of Progress in Astronautics, Academic Press, 1961.

27. Speiser, R. C., and Branson, L. K.:   Studies of a Gas Discharge Cesium Ion Source.   ARS Paper No. 2664-62, 1962.

*28. Sirois, William: Cathode Development Studies for Arc and Bombardment-Type Ion Engines.   Final Summary Report for NASA contract NAS 8-2513, Ion Physics Corp., April 1963.

*29. Hyman, J., Jr., Buckey, C. R., Eckhardt, W. O., and Knechtli, R. C.: Research Investigation of Ion Beam Formation from Electron-Bombardment Ion Sources.   Interim Technical Report on Completion of Phase I, NASA Contract NAS 3-2511, Hughes Research Labs., April 1963.

30. Reader, Paul D.: Investigation of a 10-Centimeter-Diameter Electron-Bombardment Ion Rocket. NASA TN D-1163, 1962.

31. Milder, Nelson L.: Comparative Measurements of Singly and Doubly Ionized Mercury Produced by Electron-Bombardment Ion Engine. NASA TN D-1219, 1962.

32. Mickelsen, W. R.: NASA Research on Heavy-Particle Electrostatic Thrustors. IAS Paper No. 63-19, 1963.

33. Reader, P. D.: An Electron-Bombardment Ion Rocket with a Permanent Magnet. AIAA Paper No. 63031, 1963. Also in AIAA Journal, 1963.

34. Milder, Nelson L., and Kerslake, William R.: High-Temperature Metal Filaments for Electron-Bombardment Ion Sources. Proposed NASA TN.

35. Kaufman, H. R.: The Electron-Bombardment Ion Rocket. Paper presented at AFOSR Third Symposium on Advanced Propulsion Concepts, Cincinnati, Ohio, October 2-4, 1962.

36. Kerslake, William R.: Accelerator Grid Tests on an Electron-Bombardment Ion Rocket. NASA TN D-1168, 1962.

37. Kerslake, William R., and Pawlik, Eugene V.: Additional Studies of Screen and Accelerator Grids for Electron-Bombardment Ion Thrustors. NASA TN D-1411, 1963.

38. Kerslake, W. R.: Charge-Exchange Effects on the Accelerator Impingement of an Electron-Bombardment Ion Rocket. NASA TN D-1657, 1963.

39. Speiser, R. C., and Vernon, R. H.: Cesium Ion-Atom Charge Exchange Scattering. ARS Paper No. 2068-61, 1961.

40. Kuskevics, G., Speiser, R. C., Worlock, R. M., and Zuccaro, D.: Ionization, Emission, and Collision Processes in the Cesium Ion Engine. ARS Paper No. 2364-62, 1962.

41. Stuhlinger, E.: Possibilities of Electrical Space Ship Propulsion. Report of Fifth International Astronautical Congress (1954), Vienna, Springer Publishing, 1955.

42. Stuhlinger, E.: Electric Propulsion System for Space Ships with Nuclear Power Source. Journal of Astronautics, vol. 2, 1955, p. 149; vol. 3, 1956, pp. 11 and 33.

43. Naiditch, S., Worlock, R. M., Zuccaro, D., Baker, D., Ernstene, M. P., Gallagher, L. R., and Mullins, J.: Ion Propulsion Systems: Experimental Studies. ARS Paper No. 928-59, 1959.

44. Dulgeroff, C. R., Speiser, R. C., and Forrester, A. T.: Experimental Studies with Small Scale Ion Motors. ARS Paper No. 926-59, 1959.

45. Ernstene, M. P., Forrester, A. T., Speiser, R. C., and Worlock, R. M.: Multiple Beam Ion Motors. ARS Paper No. 1373-60, 1960.

46. Ernstene, M. P., Forrester, A. T., James, E. L., Telel, D., and Worlock, R. M.: Development of High Efficiency Cesium Ion Engines. ARS Paper No. 61-83-1777, 1961.

47. Toms, R. S. H., Ernstene, M. P., Kalensher, B. E., and Selg, G. R.: Space Testing of Ion Engines. ARS Paper No. 2182-61, 1961.

48. Densmore, J. E., Tanguay, R. R., and Wilner, B. M.: Development of Ion Thrustor Systems for Space Flight Testing. ARS Paper No. 2369-62, 1962.

49. Brewer, G. R., Etter, J. E., and Anderson, J. R.: Design and Performance of Small Ion Engines. ARS Paper No. 1125-60, 1960.

50. Etter, J. E., Eilenberg, S. L., Anderson, J. R., Ward, J. W., and Brewer, G. R.: The Development of a Flight Test Ion Engine. ARS Paper No. 61-81-1775, 1961.

51. Brewer, G. R., and Work, G. A.: An Ion Engine System for Flight Testing. AIEE Conference Paper No. CP62-1162, 1962.

52. Hubach, R. A.: Limitations on the Space Test of a Cesium Ion Engine at Altitudes Below 1500 Kilometers. ARS Paper No. 2366-62, 1962.

53. Stribling, M. D., and Etter, J. E.: Recent Results on the Development of Cesium Ion Engines. AIAA Paper No. 63028, 1963.

54. Lockwood, David L., and Hamza, Vladimir: Space-Charge Flow Theory and Electrode Design for Electrostatic Rocket Engines. NASA TN D-1461, 1962.

55. Hamza, Vladimir, and Richley, Edward A.: Numerical Solution of Two-Dimensional Poisson Equation: Theory and Application to Electrostatic-Ion-Engine Analysis. NASA TN D-1323, 1963.

56. Hamza, Vladimir: Numerical Solution of Axially-Symmetric Poisson Equation; Theory and Application to Ion-Thrustor Analysis. NASA TN D-1711, 1963.

57. Wasserbauer, J. F.: Experimental Performance of a High Current Density Cylindrical Concave Porous Tungsten Emitter for Ion Engines. AIAA Paper No. 63029, 1963.

58. Reynolds, T. W., and Richley, E. A.: Thermionic Emission from Cesium-Coated Electrostatic Ion-Thrustor Electrodes. NASA TN D-1879, 1963.

59. Nazarian, G. M., and Shelton, H.: Theory of Ion Emission from Porous Media. ARS Paper No. 1386-60, 1960.

60. Zuccaro, D., Speiser, R. C., and Teem, J. M.: Characteristics of Porous Surface Ionizers. ARS Paper No. 1387-60, 1960.

61. Reynolds, T. W., and Kreps, L. W.: Gas Flow, Emittance, and Ion Current Capabilities of Porous Tungsten. NASA TN D-871, 1961.

62. Husman, O. K.: Experimental Evaluation of Porous Materials for Surface Ionization of Cesium and Potassium. ARS Paper No. 2359-62, 1962.

63. Shelton, H.: Experiments on Atom and Ion Emission from Porous Tungsten. ARS Paper No. 2360-62, 1962.

64. Husman, D. K.: A Comparison of the Contact Ionization of Cesium on Tungsten with that of Molybdenum, Tantalum, and Rhenium Surfaces. AIAA Paper No. 63019, 1963.

65. Kuskevics, G., and Thompson, B. L.: Comparison of Commercial, Spherical Powder and Wire Bundle Tungsten Ionizers. AIAA Paper No. 63016, 1963.

66. Wilson, R. G., Seele, G. D., and Hon, J. F.: Surface Ionization of Cesium with Porous Tungsten Ionizers. AIAA Paper No. 63017, 1963.

67. Teem, J. M., and Brewer, G. R.: Current Status and Prospects of Ion Propulsion. ARS Paper No. 2650-62, 1962.

68. Anglin, A. E., Jr.: Problems of Porous Tungsten Ionizers for Cesium Electric Propulsion Systems. Paper Presented at National Society of Aerospace and Process Engineers, Spring Symposium on Space Power Systems Materials, Philadelphia, Pennsylvania, June 3-5, 1963.

69. Mickelsen, W. R.: Theoretical Performance of Electrostatic Thrustors with Analytic Space-Charge Flows. NASA TR R-174, 1963.

70. Dangle, E. E., and Lockwood, D. L.: NASA Experimental Research with Ion Rockets. ARS Paper No. 1126-60, 1960.

71. Childs, J. H.: Theoretical Performance of Reverse-Feed Cesium Ion Engines. NASA TN D-876, 1961.

72. Reynolds, T. W., and Childs, J. H.: A Comparison of Reverse-Feed and Porous-Tungsten Ion Engines. NASA TN D-1166, 1962.

73. Cox, A. L., and Harrison, S.: The Controlled-Growth Colloidal Ion Source. AIAA Paper No. 63049, 1963.

74. Singer, S., Kim, N. G., and Farber, M.: An Experimental Study of Colloidal Propulsion Using Sub-Micron Particles. AIAA Paper No. 63052, 1963.

75. Krohn, V. E., Jr.: Liquid Metal Drops for Heavy Particle Propulsion. ARS Paper No. 1375-60, 1960.

76. Krohn, V. E., Jr.: Glycerol Droplets for Electrostatic Propulsion. ARS Paper No. 2398-62, 1962.

77. Hendricks, C. D., Jr., Carson, R. S., Hogan, J. J., and Schneider, J. M.: Photomicrography of Electrically Sprayed Heavy Particles. AIAA Paper No. 63051, 1963.

78. Hendricks, C. D.: Physics of Charged Colloidal Particles and the Technology of Their Production. Paper Presented at AGARD Combustion and Propulsion Panel, Athens, Greece, July 15-17, 1963.

79. Jamba, D. M., and Hornstein, B.: Charging and Removal of Surface-Condensed Particles for Colloid Propulsion. AIAA Paper No. 63053, 1963.

80. Norgren, C. T.: Onboard Colloidal Particle Generator for Electrostatic Engines. ARS Paper No. 2380-62, 1962.

81. Goldin, D. S., and Norgren, C. T.: Thrust Measurements of Colloidal

   Particles as an Indication of Particle Size and Thrustor Operation.

   AIAA Paper No. 63050, 1963.

*82. Gignoux, D., Einbinder, H., and Anton, H.: Nozzle for Colloidal

   Propulsion, Analytical Investigation. Final Report, Phase I,

   NASA Contract No. NASr-45, Cosmic, Inc., August 1961.

---

*Some of these reports will be available only to agencies of the
United States Government and their contractors, while others may become
available for general distribution in the future.
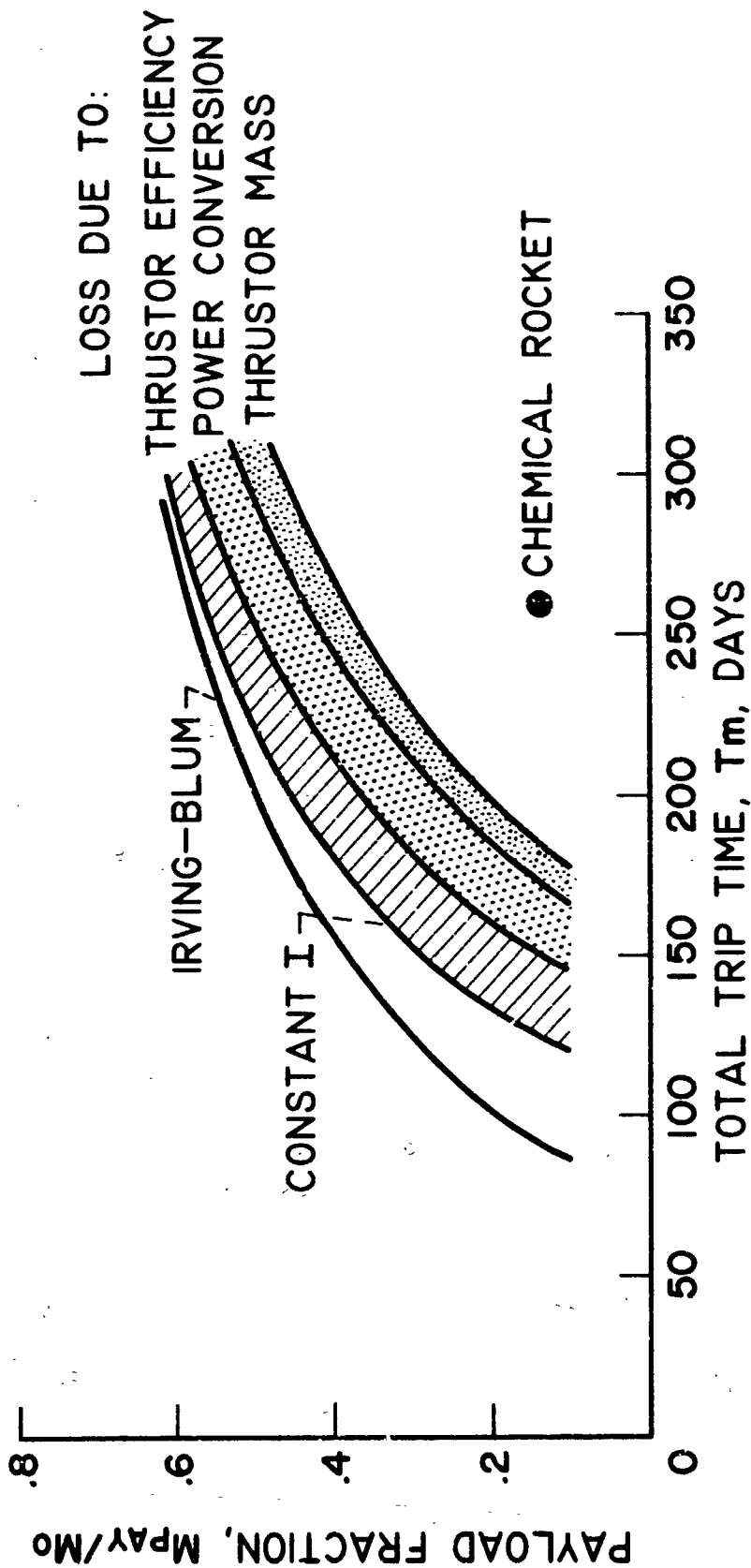
Fig. 1. - Payload fraction as a function of trip time for Mars orbiter mission.
Basic electric powerplant weight, 4 KG/KW.

PROPELLANT

HIGH
POTENTIAL

SPACE POTENTIAL

IONS

ELECTRONS

IONIZER

ELECTRIC-
POWER
GENERATOR
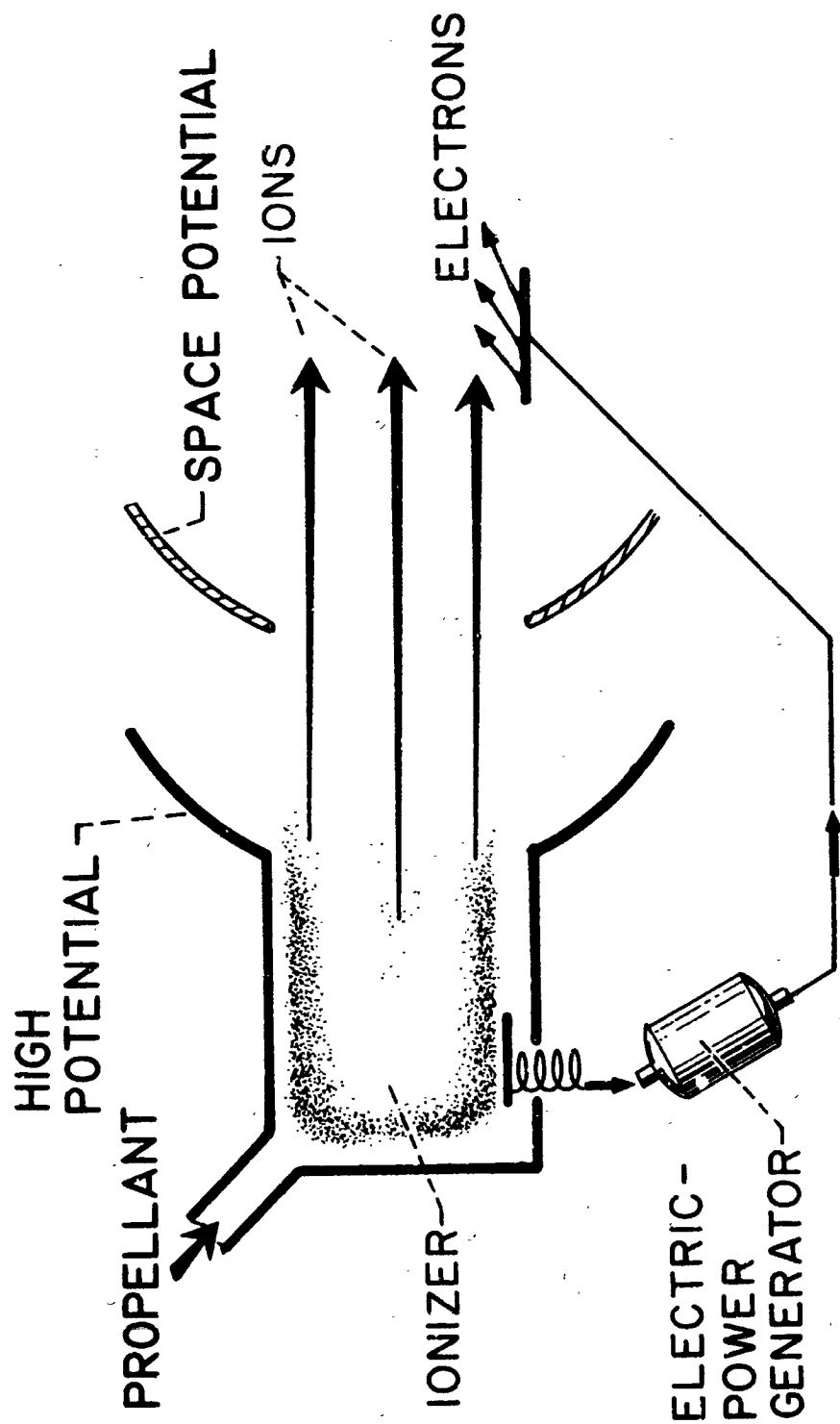
Fig. 2. - Schematic drawing of electrostatic thrustor.
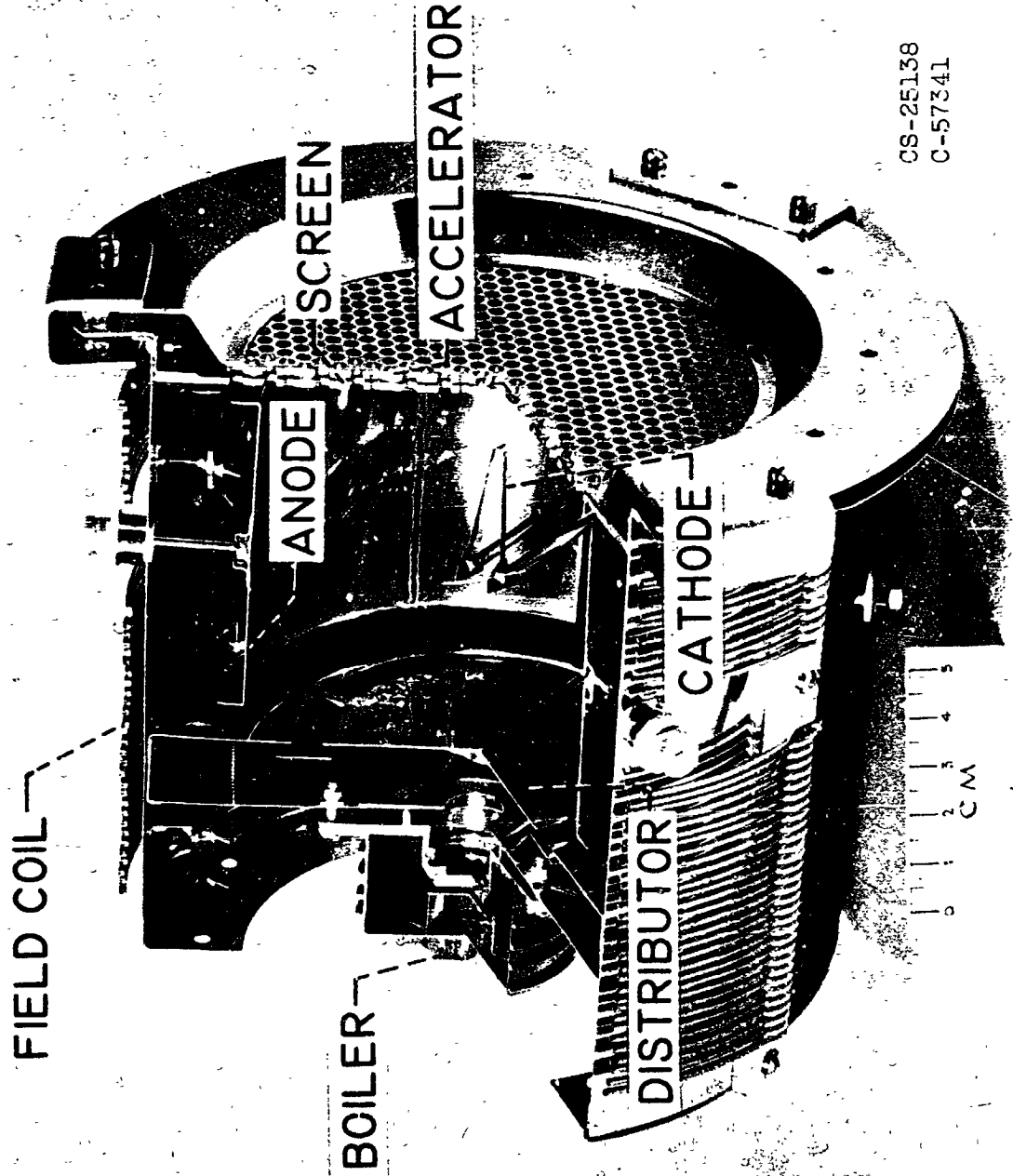
CS-25138
C-57341

Fig. 3. - Electron-bombardment thrustor for mercury propellant.
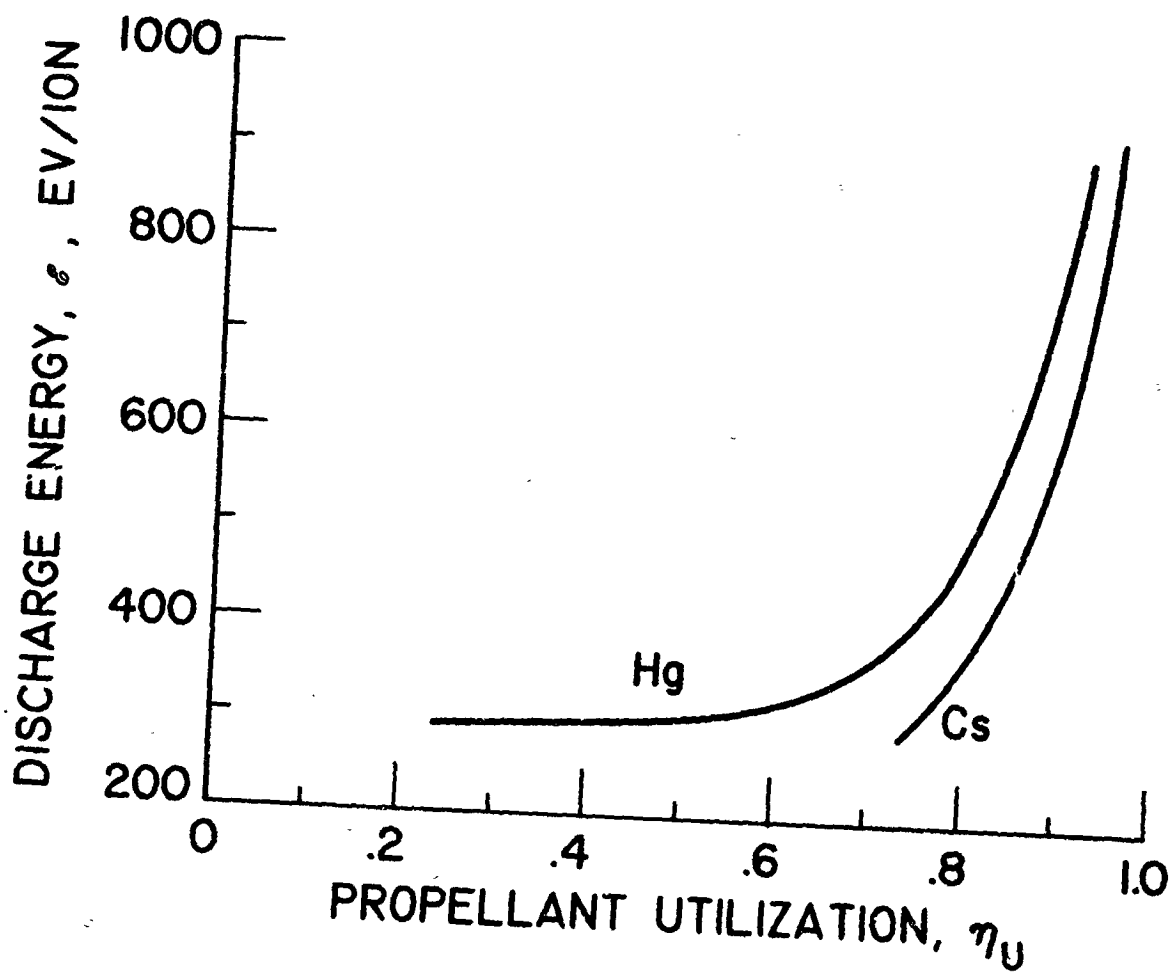
Fig. 4. - Ion-chamber losses as a function of propellant utilization.
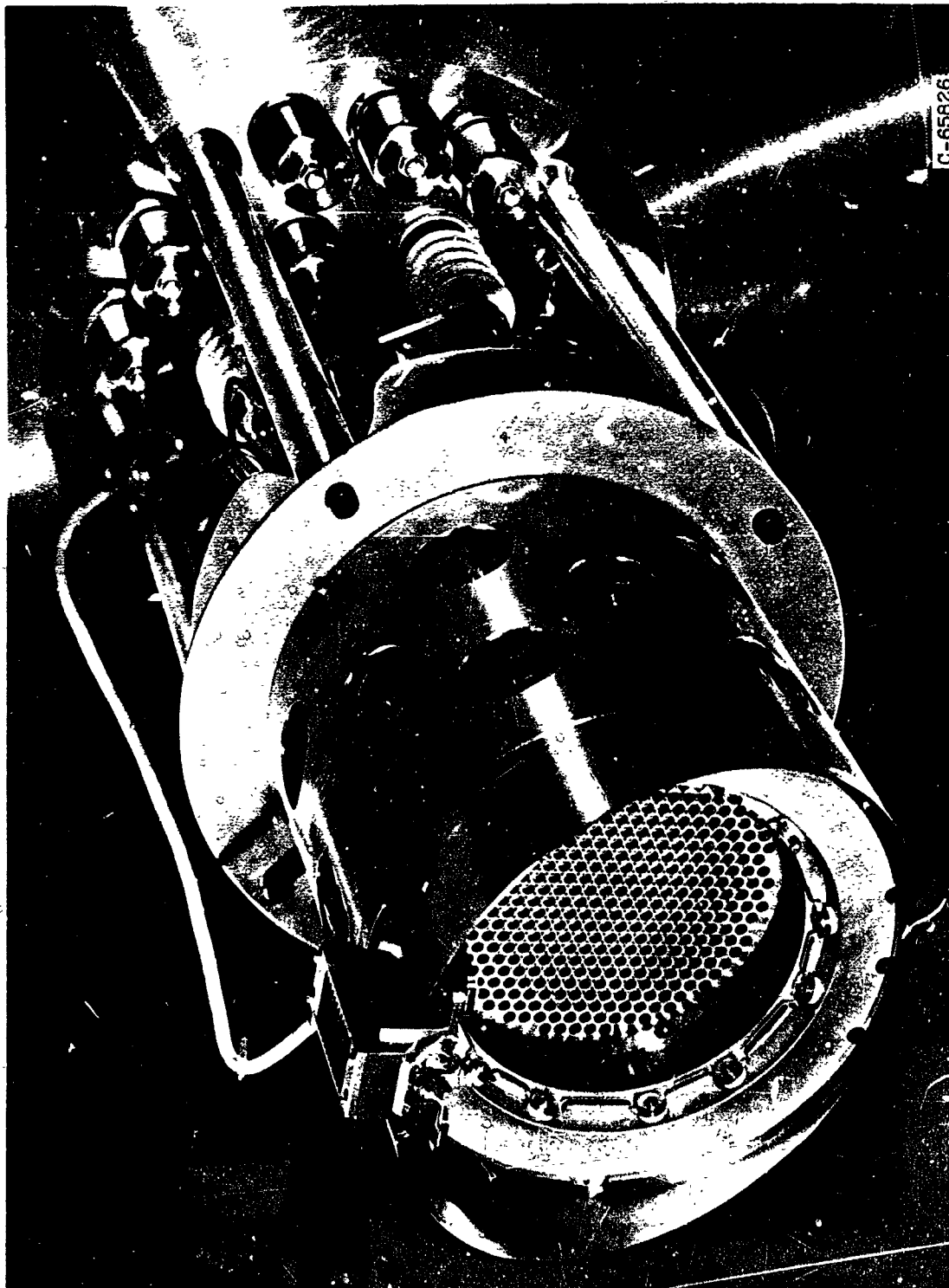
C-65826

Fig. 5. - Electron bombardment thrustor designed at Electro-Optical Systems, Inc. for Cesium propellant.

INCHES
0   1   2

C-65360
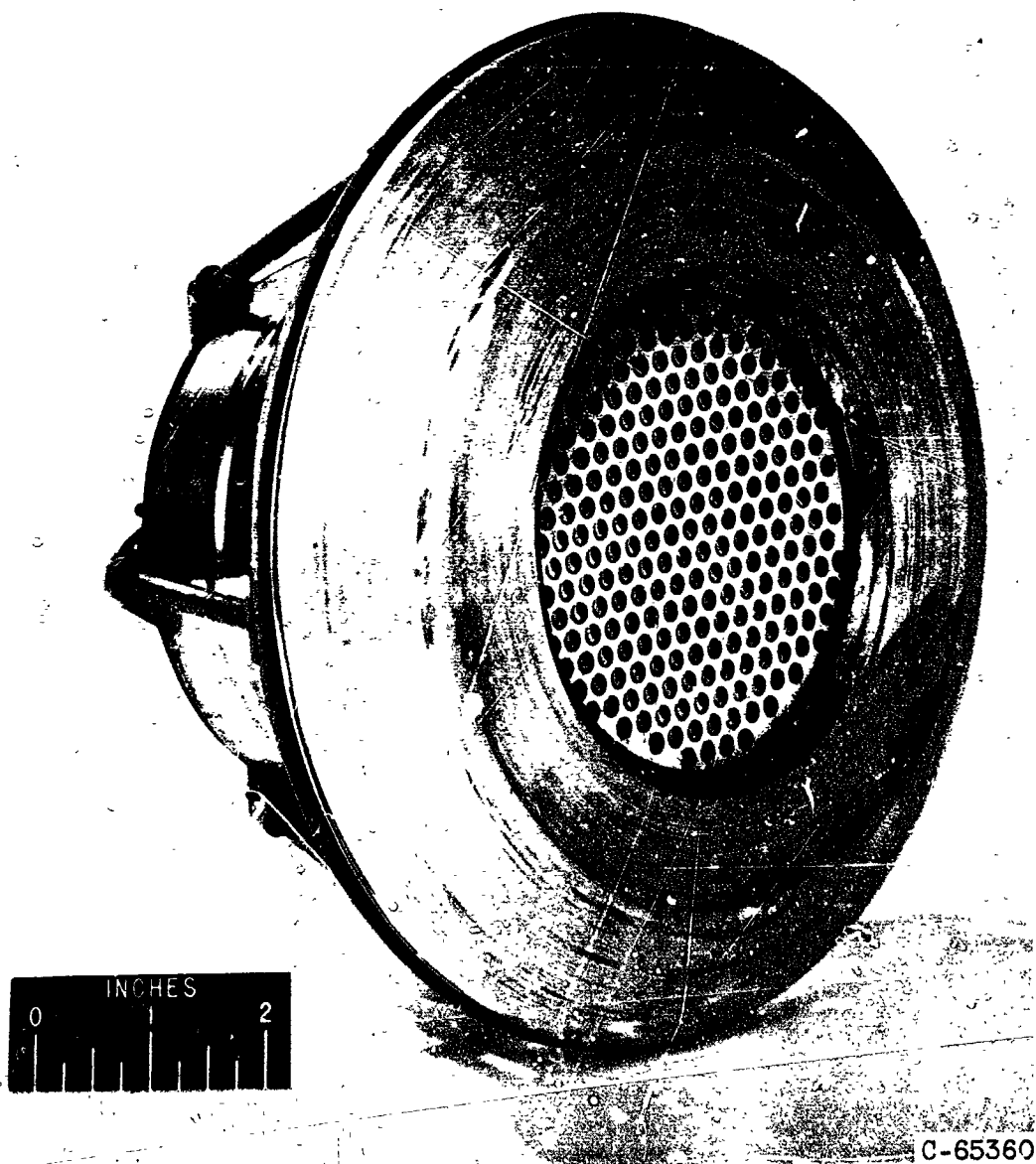
Fig. 6. - Permanent-magnet 10-cm module of electron-bombardment
thrustor designed at the NASA Lewis Laboratory for mercury
propellant.
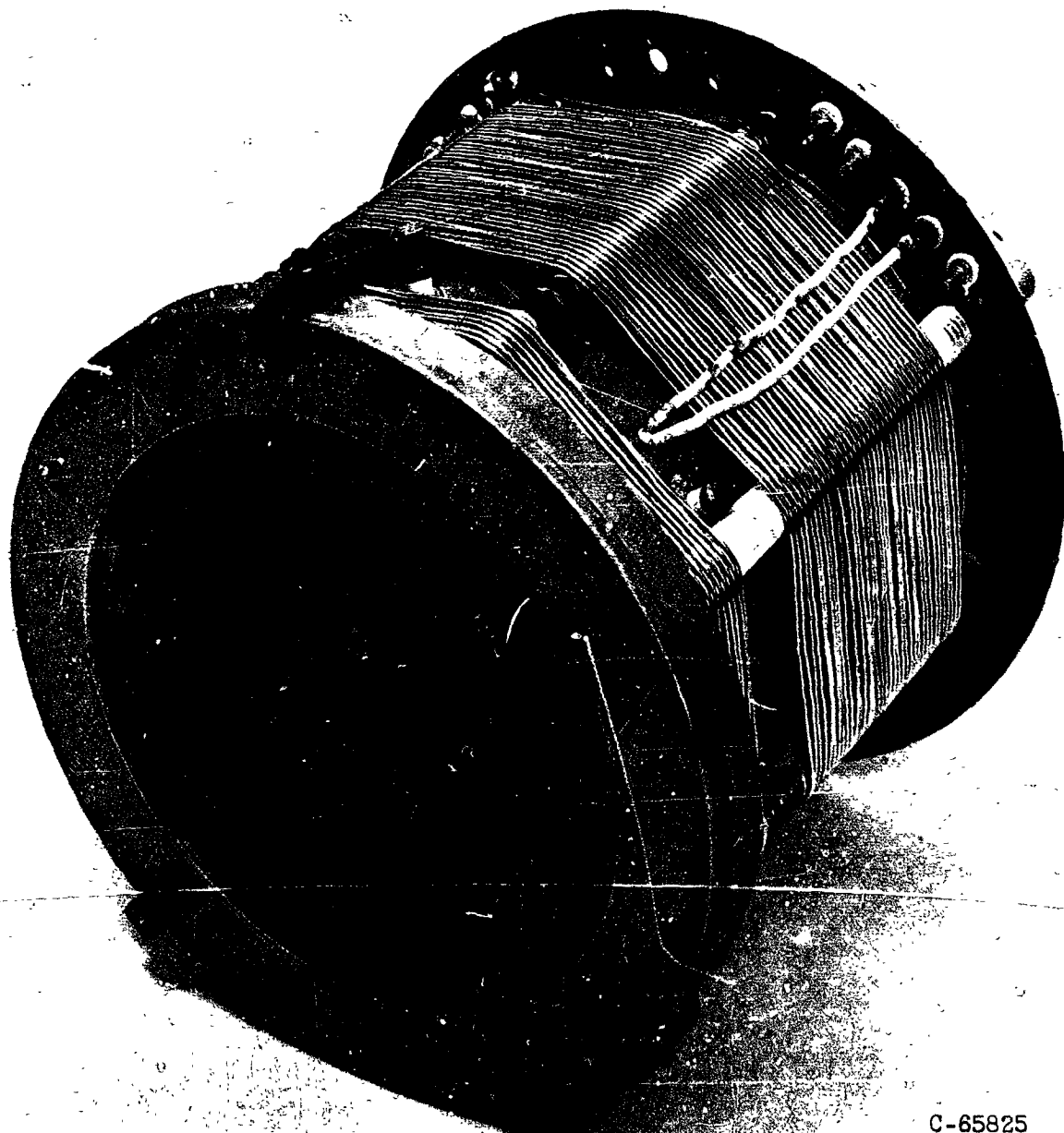
C-65825

Fig. 7. - Electron-bombardment thrustor designed at Ion Physics Corp.
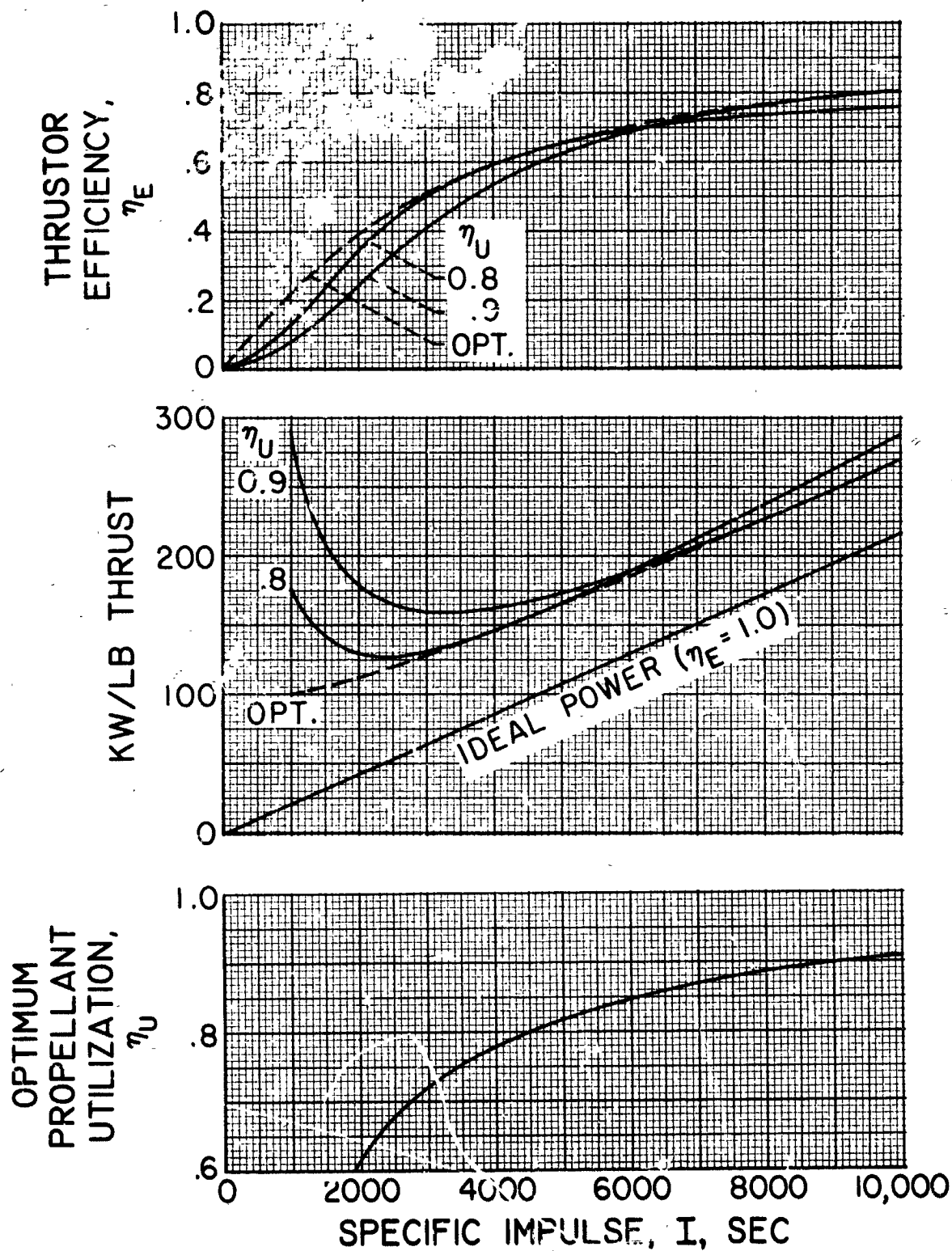
Fig. 8. - Estimated performance of electron-bombardment thrustor with mercury propellant.
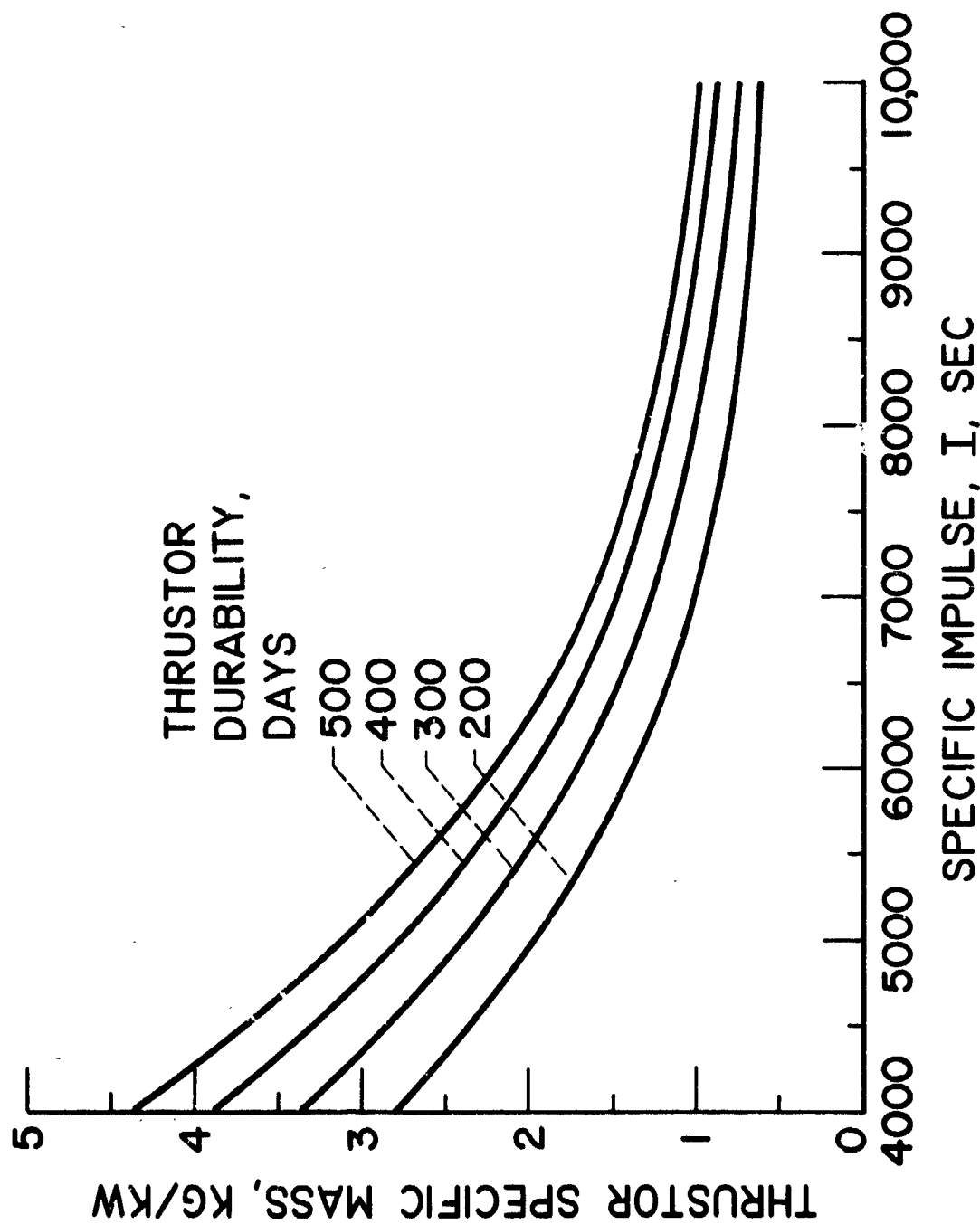
Fig. 9. - Specific mass of electron-bombardment thrustor assuming adequate cathode durability.

ELECTRONS

CESIUM IONS

HOT
TUNGSTEN
IONIZER

NEUTRAL
CESIUM
ATOMS

CS-26247
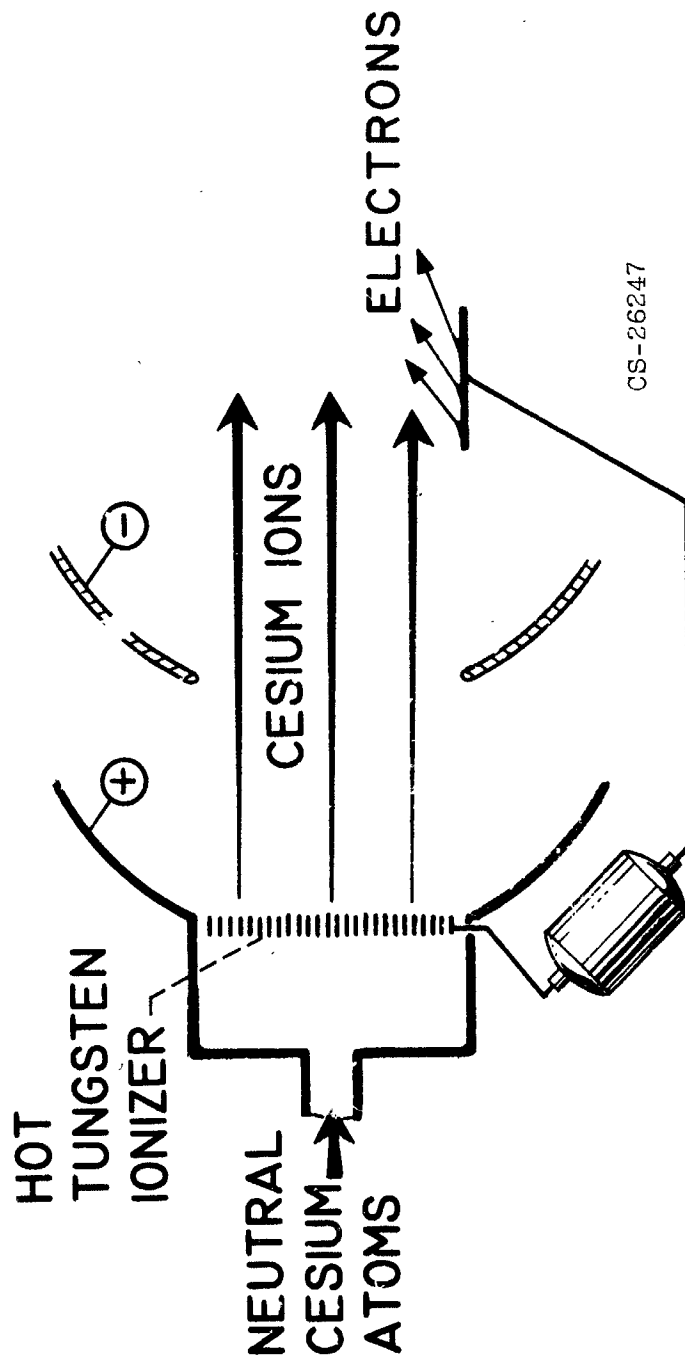
Fig. 10. – Schematic drawing of contact-ionization thrustor.

are described in references 43 to 48, and a photograph of one of the design versions is shown in figure 11. Another type of contact-ionization thrustor is under development at Hughes Research Laboratory. The progress and performance of this thrustor are described in references 49 to 53, and a photograph of one of the design versions is shown in figure 12.

Both of these thrustors are based on common fundamentals, so they will be discussed concurrently. Both have porous wolfram ionizers. By virtue of its own vapor pressure, cesium diffuses through the pores of the ionizer and is ionized by contact on the "downstream" face of the ionizer. The cesium ions are then accelerated by the accelerator electrodes. The cesium ions are singly charged, so their final speed is uniform.

The major power loss in these thrustors is due to thermal radiation from the ionizer. Conduction heat loss has been minimized, and the "upstream" side of the ionizer and propellant-feed manifolds are well insulated to minimize thermal-radiation loss. The accel length has been made as short as presently possible and is only a few millimeters in both thrustor concepts.

As shown in figures 11 and 12, the EOS thrustor consists of an array of ionizer "buttons" and circular electrode apertures, while the Hughes thrustor consists of concentric "annular" ionizers and exhaust apertures. Both thrustors have concave ionizer surfaces but different electrode shapes. The neutralizer designs are also different.

C-65824

Fig. 11. - Contact-ionization thrustor designed at Electro-Optical Systems, Inc.

C-65823

Fig. 12. - Contact-ionization thrustor designed at Hughes Research Laboratory.

BEAM-FORMING
ELECTRODE

ACCEL
ELECTRODE

BEAM EDGE

CHARGE-EXCHANGE
ION TRAJECTORIES

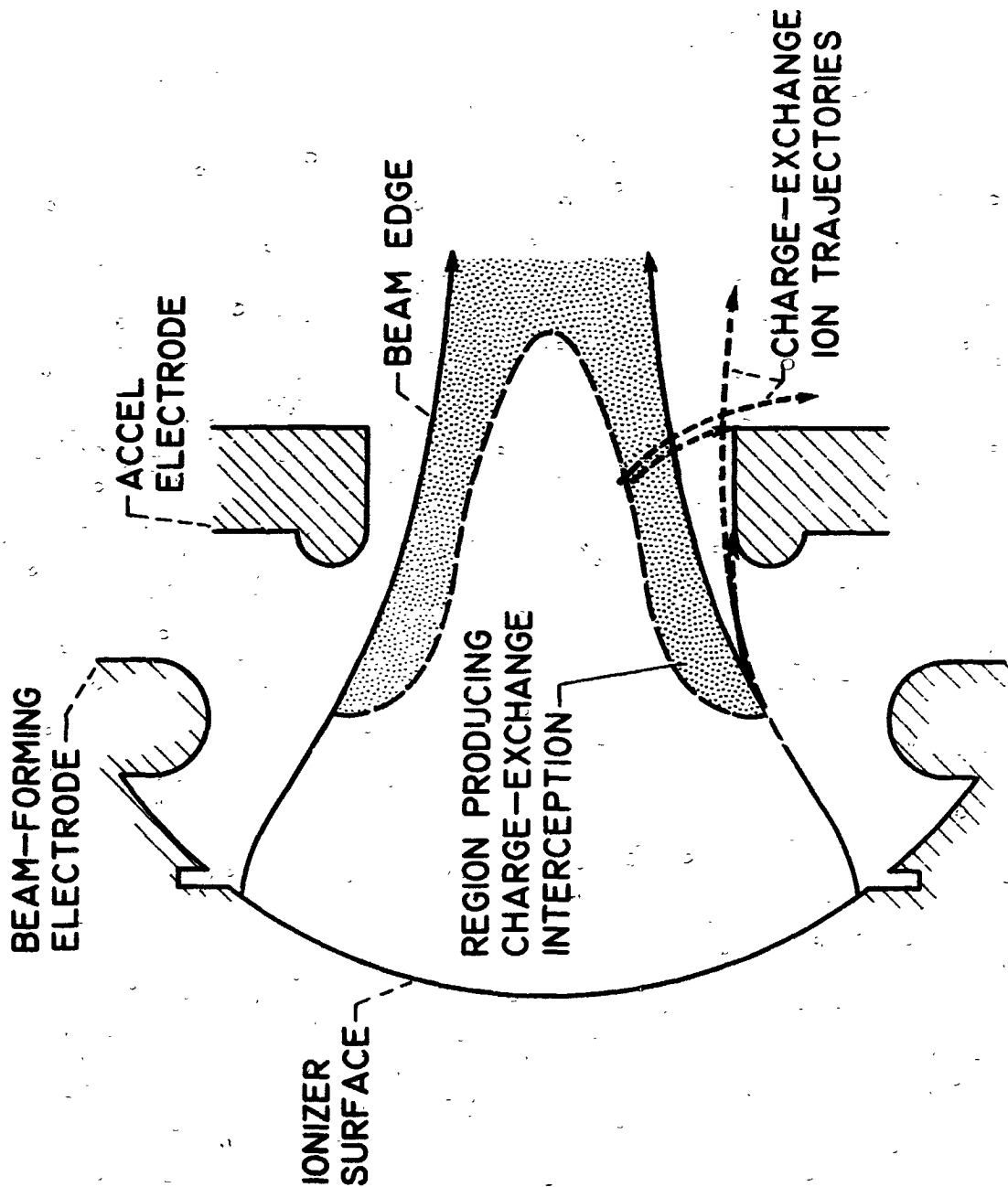REGION PRODUCING
CHARGE-EXCHANGE
INTERCEPTION

IONIZER
SURFACE

Fig. 13. - Theoretical analysis of charge-exchange ion trajectories.
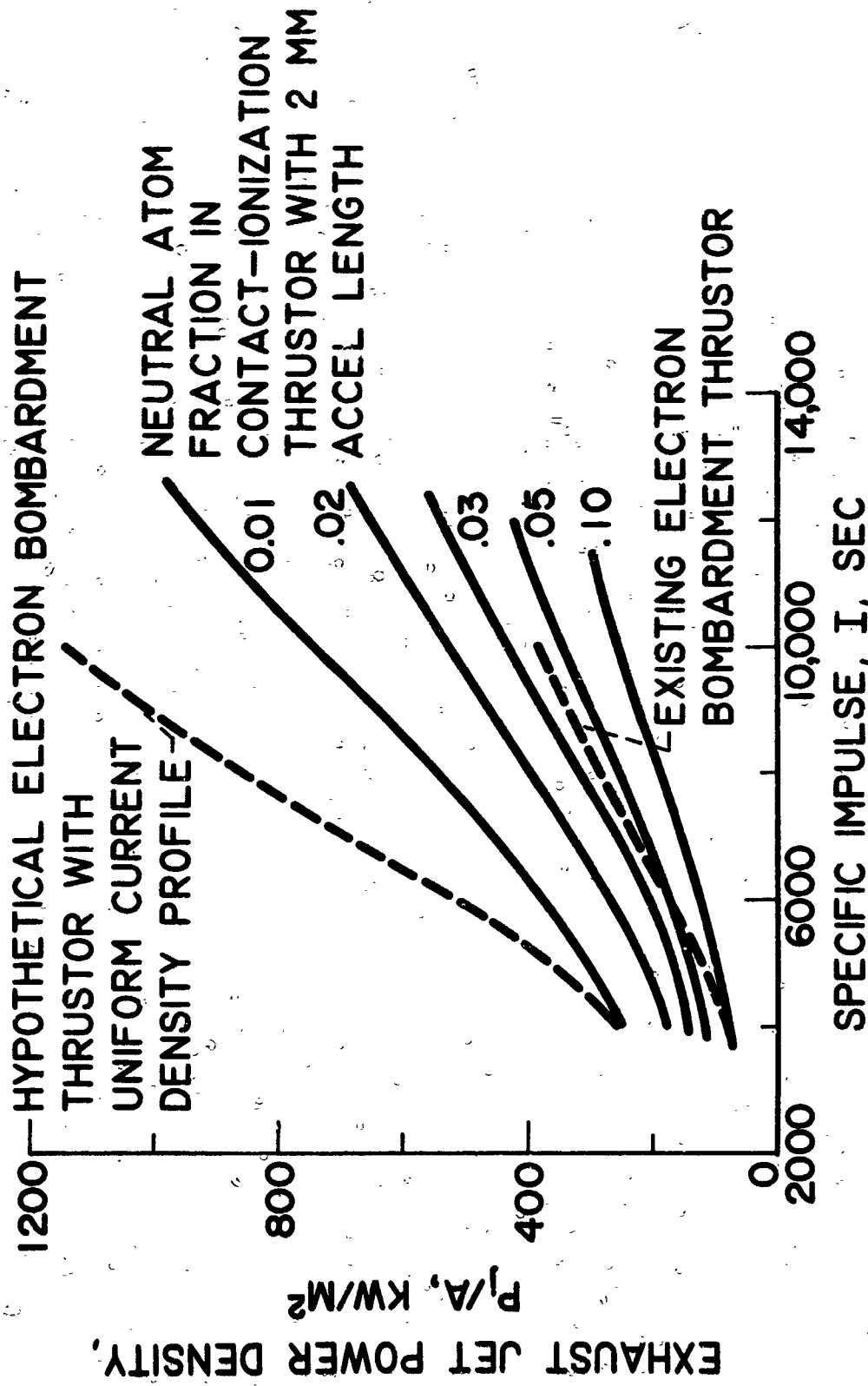
Fig. 14. - 400 day durability limits on exhaust-jet power density due to charge-exchange ion erosion of the accel electrode. Contact-ionization thrustor, copper electrode. Electron-bombardment thrustor, molybdenum electrode.

SURFACE DIFFUSION ⌐KNUDSEN FLOW

→ IONS

CROSS SECTION END VIEW
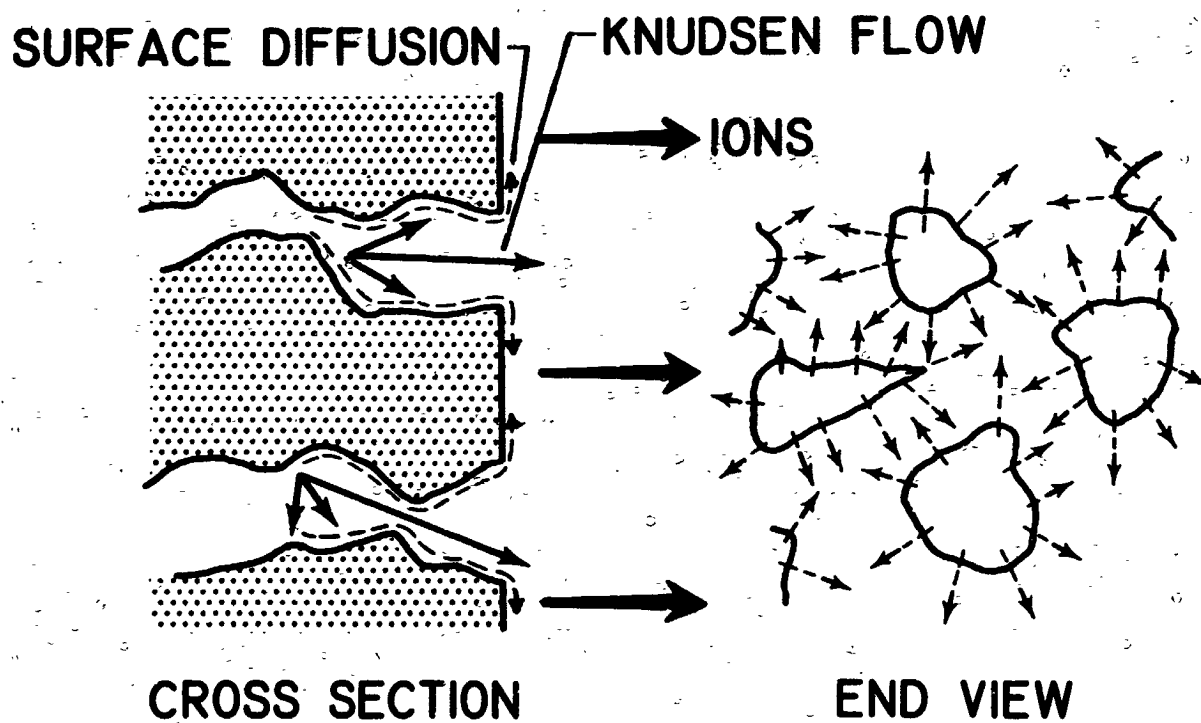
Fig. 15. - Schematic drawing of flow through porous wolfram.
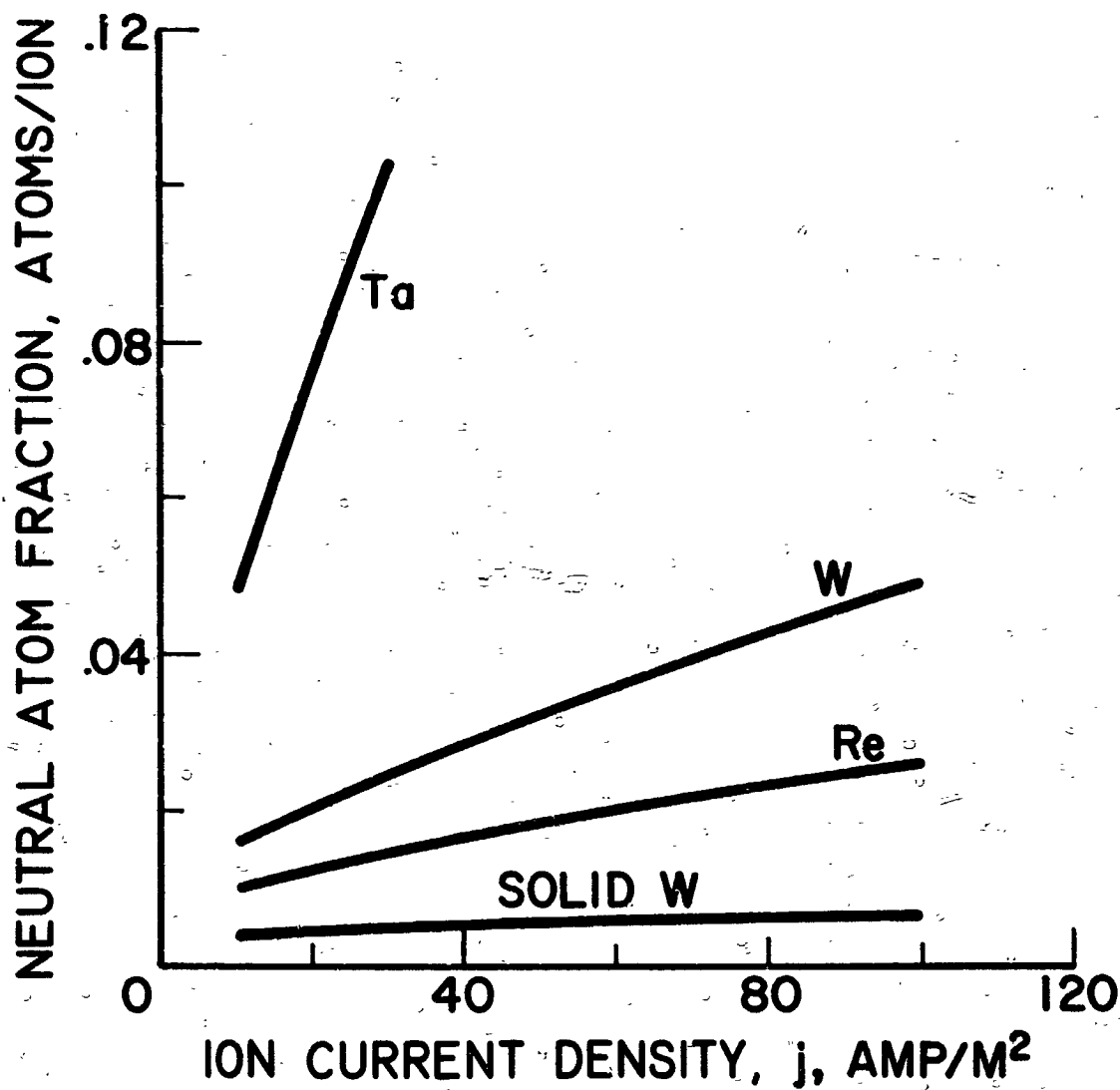
Fig. 16. - Neutral-atom efflux from various porous ionizers.
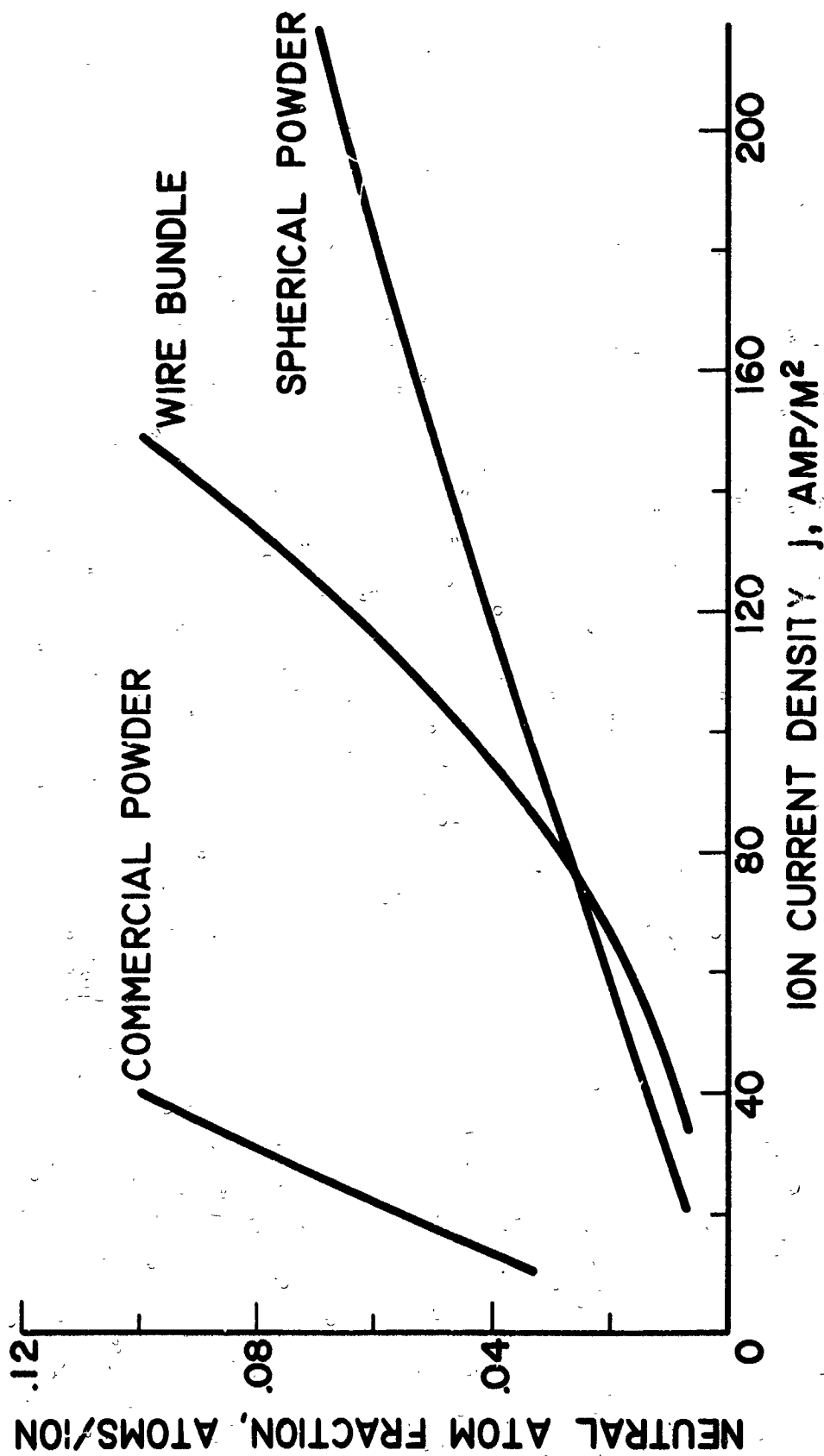
Fig. 17. - Neutral-atom efflux from porous wolfram ionizers.

E-2238
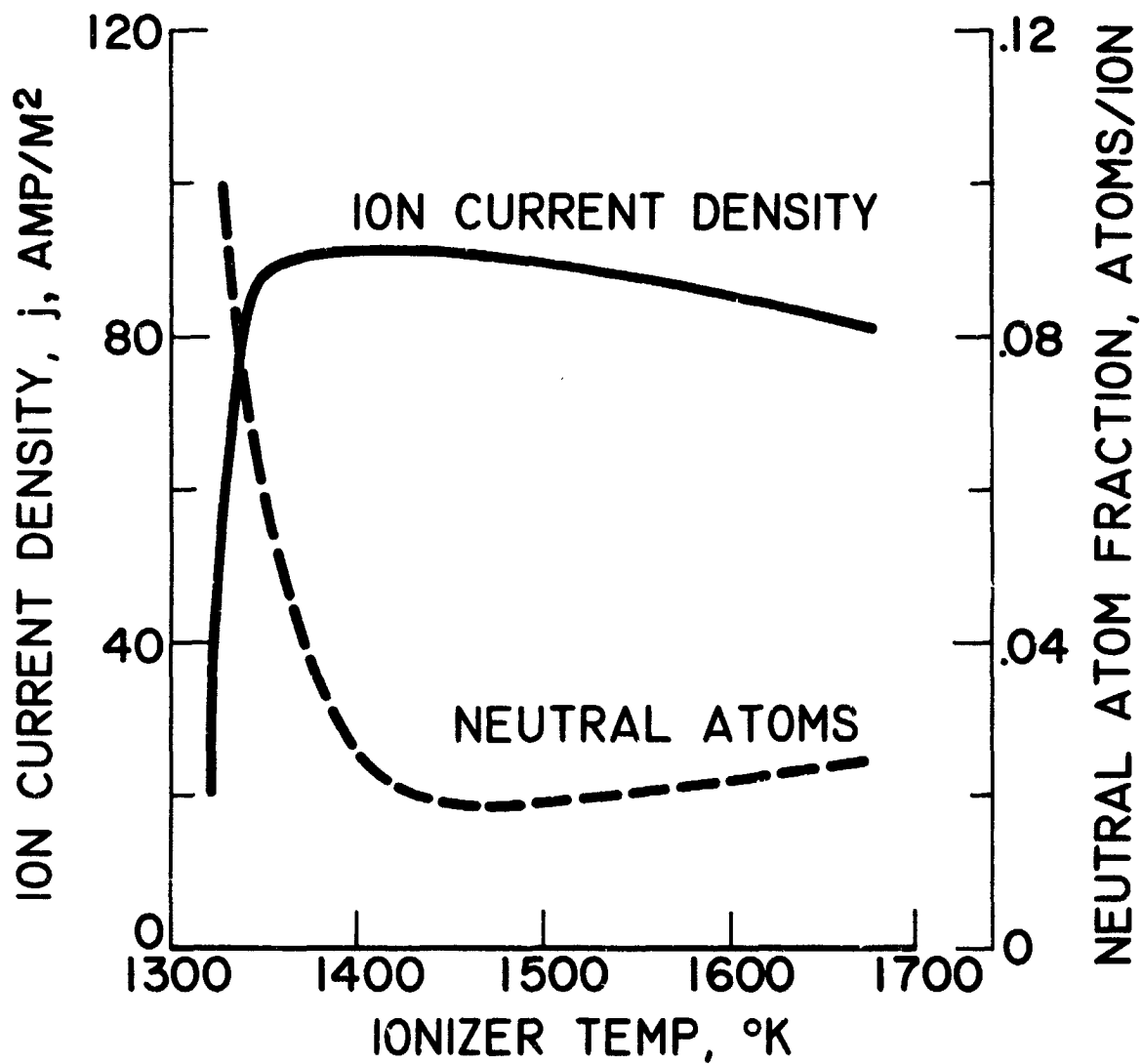
Fig. 18. - Effect of ionizer temperature on ion cur-
rent density and neutral-atom efflux from porous-
wolfram ionizer.
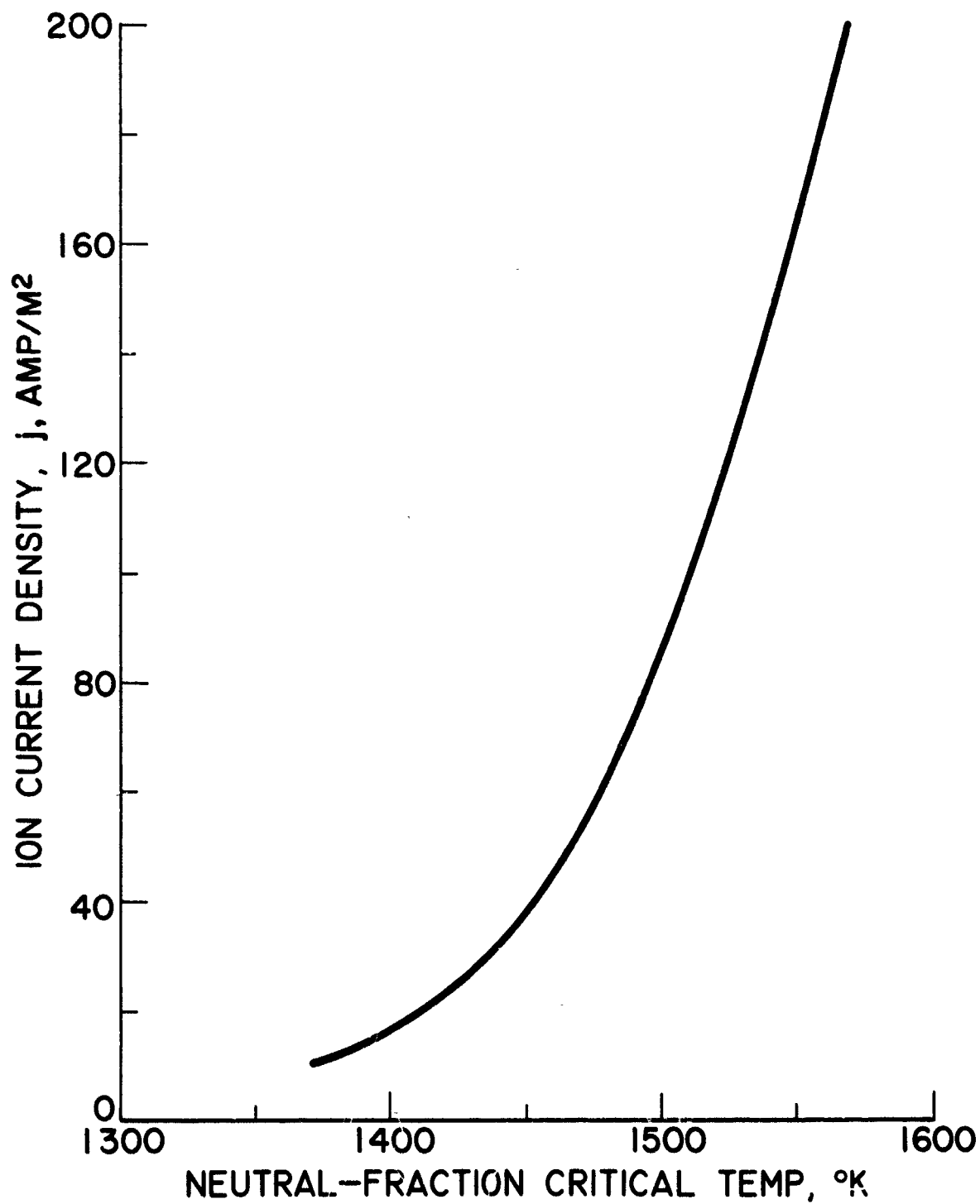
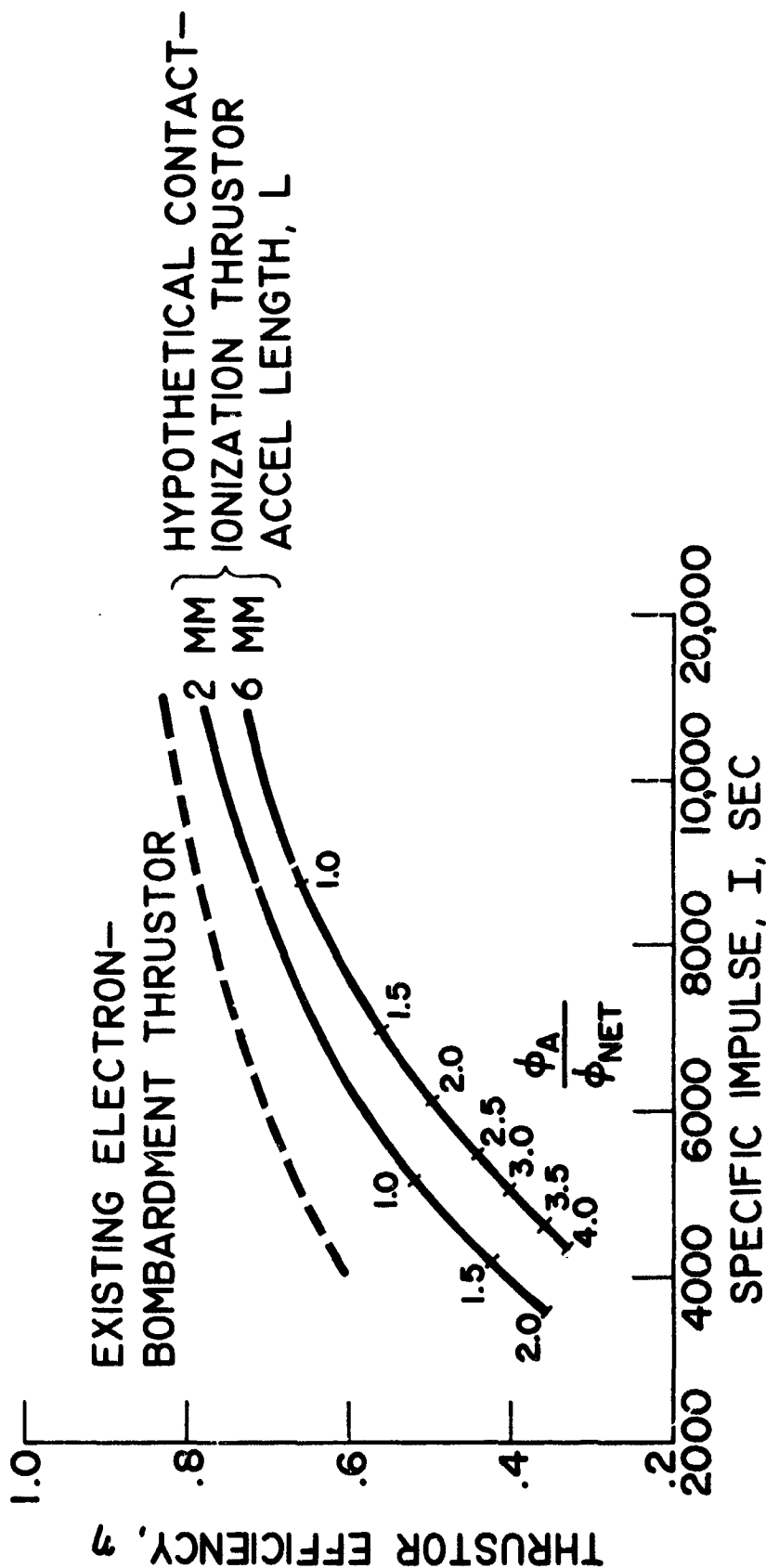Fig. 19. - Neutral-fraction critical temperature for spherical powder porous-wolfram ionizers.

Fig. 20. - Estimated limitation on thrustor efficiency due to charge-exchange ion erosion of copper accel electrode. 400-day durability. Spherical powder porous-wolfram ionizer.
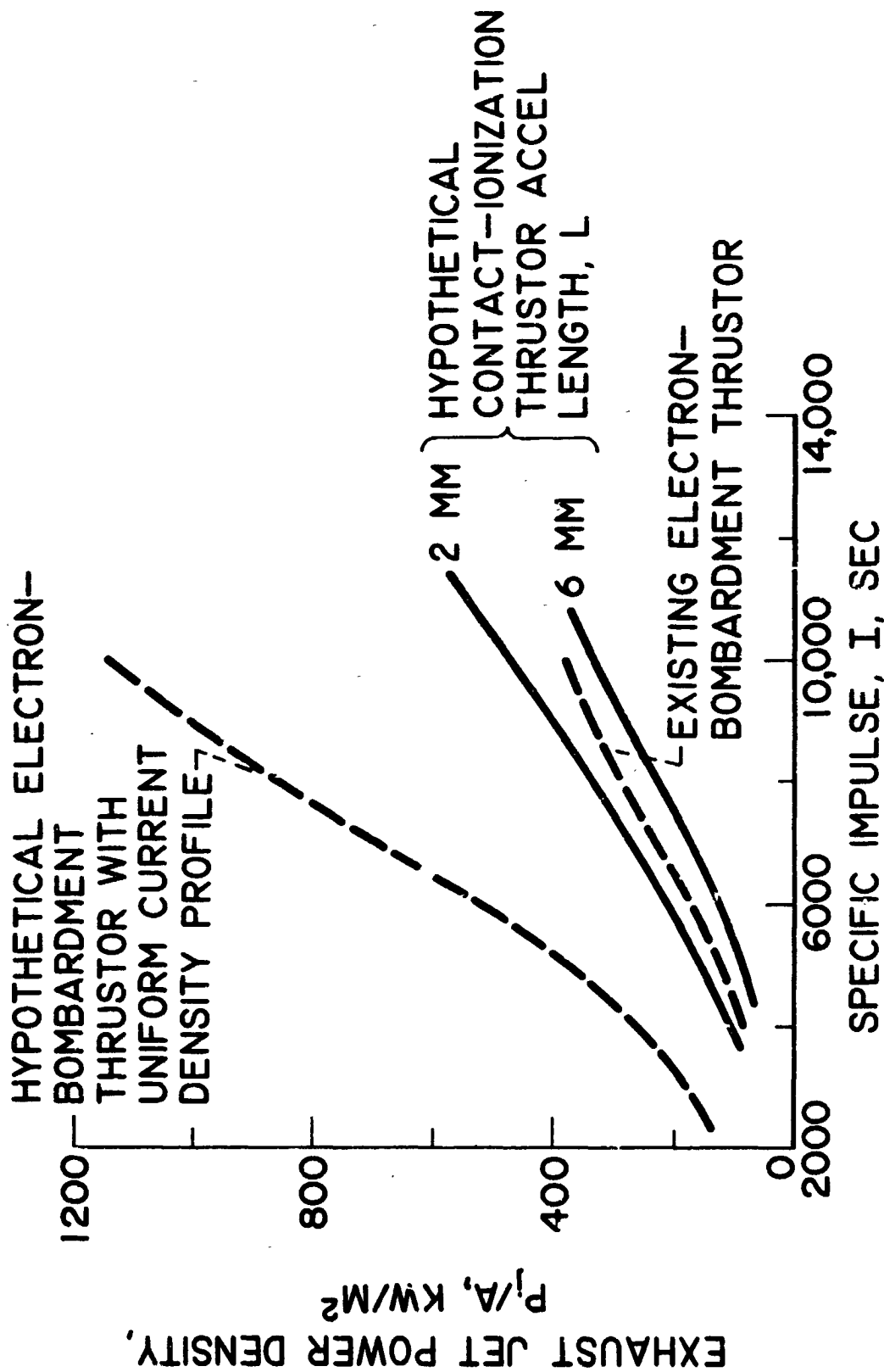
Fig. 21. - Exhaust-jet power density limitations for hypothetical contact-ionization thrusters with spherical powder porous-wolfram ionizers and 400-day durability.
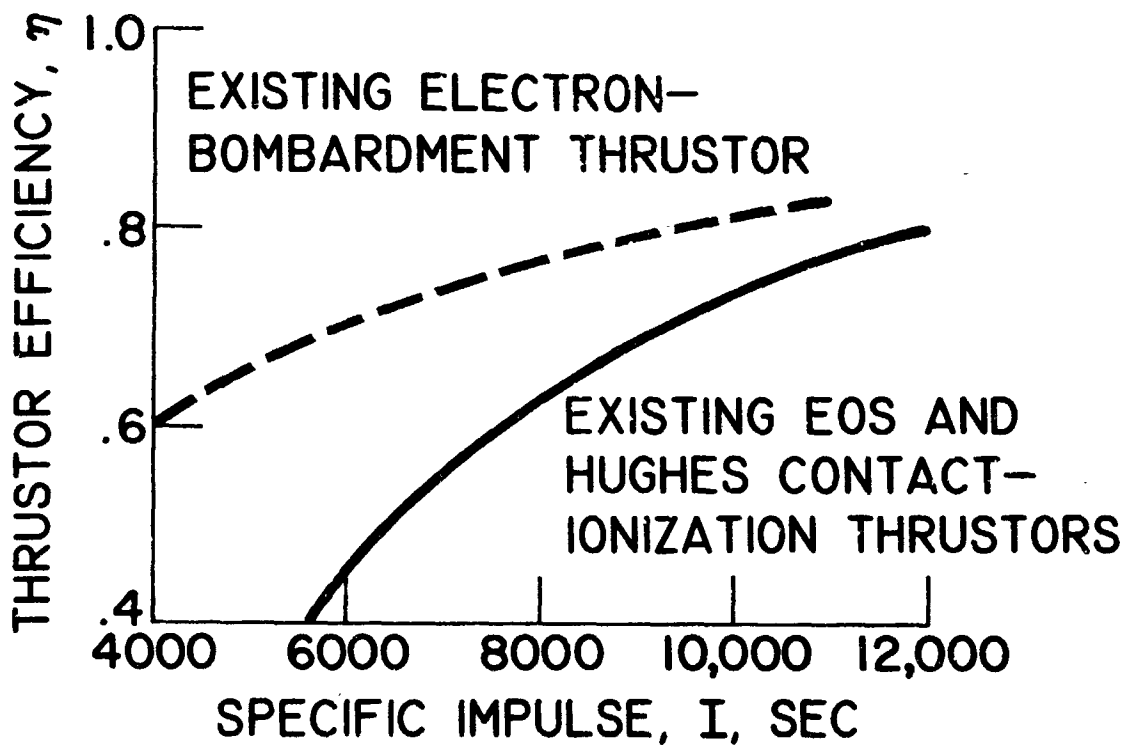
Fig. 22. - Efficiency of existing EOS and Hughes contact-ionization thrustors (uncorrected for durability).
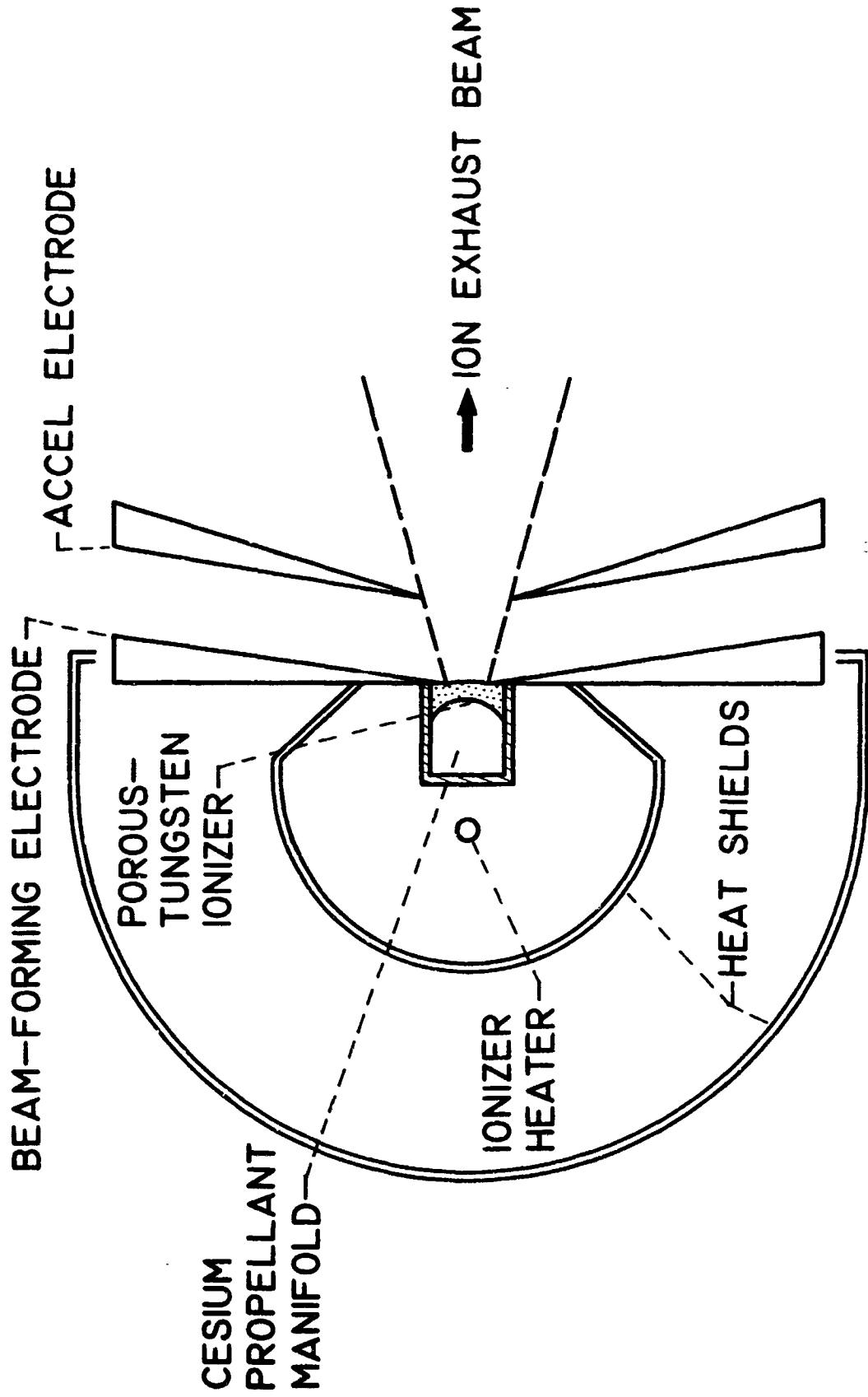
Fig. 23. - Divergent-flow contact-ionization thrustor designed at the NASA Lewis Laboratory. Ionizer height, 101 mm; ionizer chord, 1.5 mm; ionizer radius, 3 mm; exhaust aperture radius, 6 mm.
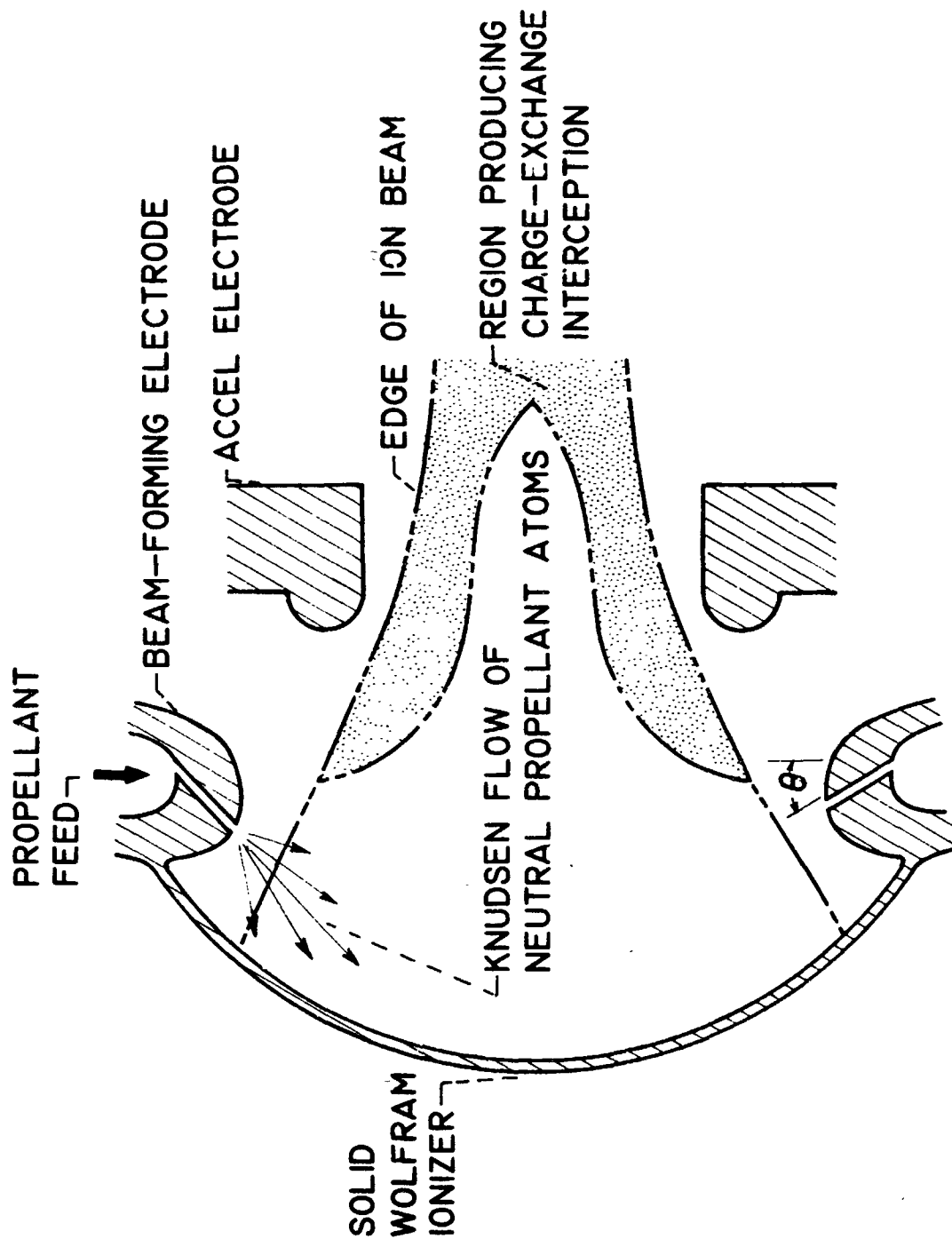
PROPELLANT FEED

BEAM-FORMING ELECTRODE

ACCEL ELECTRODE

EDGE OF ION BEAM

REGION PRODUCING CHARGE–EXCHANGE INTERCEPTION

KNUDSEN FLOW OF NEUTRAL PROPELLANT ATOMS

SOLID WOLFRAM IONIZER

θ

Fig. 24. – Hypothetical design for reverse-feed contact-ionization thrustor.